Quaternary Science Reviews 124 (2015) 106–123

Contents lists available at ScienceDirect

Quaternary Science Reviews

journal homepage: www.elsevier.com/locate/quascirev

Geomorphological evidence and ^{10}Be exposure ages for the Last Glacial Maximum and deglaciation of the Velká and Malá Studená dolina valleys in the High Tatra Mountains, central Europe

Zbyněk Engel [a, *], Pavel Mentlík [b], Régis Braucher [c], Jozef Minár [d], Laetitia Léanni [c], Aster Team[c, 1]

[a] Department of Physical Geography and Geoecology, Faculty of Science, Charles University in Prague, Albertov 6, 12843 Praha, Czech Republic
[b] Center of Biology, Geoscience and Environmental Education, University of West Bohemia, Klatovská 51, 30619 Plzeň, Czech Republic
[c] Centre Européen de Recherche et d'Enseignement en Géosciences de l'Environnement, Aix-Marseille Université, CNRS-IRD UM 34, 13545 Aix-en-Provence Cedex 4, France
[d] Department of Physical Geography and Geoecology, Faculty of Natural Sciences, Comenius University, Mlynská dolina B1, SK-842 15 Bratislava, Slovak Republic

ARTICLE INFO

Article history:
Received 18 April 2015
Received in revised form
26 June 2015
Accepted 14 July 2015
Available online xxx

Keywords:
Quaternary
Glaciation chronology
Glacier retreat
Thinning rate
Paraglacial
High Tatra Mts.
Western Carpathians

ABSTRACT

^{10}Be exposure age chronology of the last glaciation was established in a key area at the southern slopes of the High Tatra Mts., Western Carpathians. In-situ produced ^{10}Be in moraine boulders, glacially transformed bedrock surfaces and rockfall accumulations constrains the timing of the Last Glacial Maximum (LGM) glacier expansion and provides chronological evidence for the post-LGM decay of one of the largest paleoglaciers in the range. The uncertainty-weighted mean age of 22.0 ± 0.8 ka obtained for the terminal moraine in the forefield of the Velká Studená dolina Valley indicates that the oldest moraine was deposited close to the global LGM. This finding confirms that well-preserved moraines in the range were formed during the last glacial cycle and that glaciation on the southern flank of the range was more extensive than earlier in the last glacial cycle. The maximum glacier extent correlates with late Würmian/Weichselian glacier phases in the Alps, the Bavarian/Bohemian Forest and the Krkonoše Mts., but probably postdates the period of maximum glaciation in the Southern Carpathians. Re-advance moraines at the mouth of the Velká Studená dolina Valley and in the middle part of the Malá Studená dolina Valley were deposited no later than around 20.5 ka and 15.5 ka, respectively. The timing of these advances is broadly synchronous within the High Tatra Mts. as well as with glacier advances in the Alps, Bavarian/Bohemian Forest and Krkonoše Mts. ^{10}Be exposure ages obtained from glacially transformed bedrock surfaces range between 20.5 ± 1.7 ka and 10.7 ± 0.3 ka constraining the onset and the final phase of the deglaciation. Surface exposure dating of four rockfall accumulations produced uncertainty-weighted mean ages of 20.2 ± 1.2 ka, 17.0 ± 0.7 ka, 16.5 ± 0.4 ka and 15.6 ± 0.7 ka. These ages indicate that activation of rock-slope failures occurred under paraglacial conditions within a few centuries up to 1400 years after the formation of re-advance moraines.

1. Introduction

The Carpathians belong to the most extensive mountain range in mainland Europe with an area of 210,000 km^2 and a total length of 1500 km (UNEP, 2007). The Carpathian arc extends from the eastern margin of the Alps to the Balkan Peninsula spanning a considerable area in both latitude (44–50° N) and longitude (17–27° E). A number of former glaciers within the Carpathians offer an opportunity for the investigation of climatic conditions across a large area between the central European uplands and the Black Sea during past glaciations (e.g. Heyman et al., 2013). The former existence of glaciers in the Carpathians was first recognised in the High Tatra Mts., Western Carpathians, in the mid-19th century (Zejszner, 1856). The initial studies focused on the

* Corresponding author.
E-mail address: engel@natur.cuni.cz (Z. Engel).
[1] Aster Team: Maurice Arnold, Georges Aumaître, Didier Bourlès, Karim Keddadouche.

http://dx.doi.org/10.1016/j.quascirev.2015.07.015
0277-3791/

identification of glacial landforms and the probable extent of mountain glaciers. Most of the cirques and moraines were recognised by Partsch (1882) who also reconstructed the thickness, length and equilibrium line altitude (ELA) of local glaciers. Two contrasting hypotheses were considered for the probable extent of formerly glacierised area. Dénes (1902) suggested extensive glaciation with a piedmont glacier lobe along the southern flank of the range whereas later studies rejected this hypothesis and suggested glaciation confined to cirques and valleys (Partsch, 1923). Several glacial episodes were identified in the range based on morphological characteristics and the relative position of the moraines in the landscape. Dénes (1902) and Partsch (1907) hypothesised two or three glaciations, whereas de Martonne (1911) assigned all the moraines to the last glacial period. The hypothesis of a single glaciation was rejected and a sequence of two to four glaciations was tentatively proposed (Partsch, 1923; Romer, 1929). Subsequently, the moraines of the last glaciation were described in detail and attributed to five to seven re-advances based on geomorphologic criteria (Halicki, 1930; Lukniš, 1959; Klimaszewski, 1960; Baumgart-Kotarba and Kotarba, 1997).

Initial attempts to constrain the timing of glaciations via absolute dating occurred in the 1980s when radiocarbon dating and the pollen analysis were applied to sedimentary sequences in moraine-dammed lakes. These studies provided evidence of ice-free periods in Przedni Staw Polski Lake in the Pięciu Stawów Polskich Valley (Krupiński, 1984), Czarny and Zielony Staw Gąsienicowy Lakes in the Sucha Woda Valley (Baumgart-Kotarba and Kotarba, 1993) and Małe Żabie Oko Lake in the Rybi Potok valley (Baumgart-Kotarba and Kotarba, 1995, 1997). Glacier advances were dated based on thermoluminescence (Prószyńska-Bordas et al., 1988; Butrym et al., 1990; Lindner et al., 1990, 1993; Lindner, 1994) and optically stimulated luminescence data (Baumgart-Kotarba and Kotarba, 2001) from glacial and glaciofluvial sediments in the north-facing valleys and along the northern foreland of the range. In recent years, exposure ages allowed the reconstruction of the glacier retreat in the Sucha Woda and Pięciu Stawów Polskich/Roztoka valleys (Dzierżek et al., 1999; Baumgart-Kotarba and Kotarba, 2001; Dzierżek, 2009; Makos et al., 2013a,b; see Fig. 1 for the location).

Despite this long history of glacial research, the chronology of glaciations in the High Tatra Mts. remains poorly constrained. In particular, chronological data are available for only a few valleys and the results of different dating methods are partly contradictory. The aim of this paper is to present chronological data for the most complete sequence of moraines and related landforms in the southern part of the range, and to interpret the glacial history of this region in the light of recent studies in the Carpathians and other mountain regions in central Europe.

2. Study area

The High Tatra Mts. (49°05′–49°20′ N, 19°35′–20°25′ E), the northernmost part of the Western Carpathians, are a 26 km long and 17 km wide range. The range represents the highest part of the Carpathians reaching a maximum elevation of 2655 m above sea level (a.s.l.) at the top of Gerlachovský štít Mountain. The southern part of the range, including its main ridge, is built of Variscan granitoids which are covered with Paleogene flysch of the Liptov Trough in the south (Jurewicz, 2007). The crystalline basement is overlain by Mesozoic sedimentary sequences, which consist of an autochthonous sedimentary cover, the High-Tatric and Krížna nappes in the northern part of the range (Putiš, 1992). In an orographic sense the range emerged due to Miocene rotational uplift that resulted in the asymmetric horst structure of the massif (Králíková et al., 2014 and references therein). The asymmetry is expressed in higher elevation of the southern ridges and in generally shorter and more inclined southern valleys compared to north-facing valleys (Lukniš, 1973). The massif is deeply dissected by glacial valleys and cirques, displaying the most pronounced glacial morphology within the Carpathians. However, at present there are only glacierets, or firn-ice patches, below north-facing rock walls (Gądek, 2008).

The climate in the High Tatra Mts. is influenced mainly by maritime air masses (Niedźwiedź, 1992). The range represents an orographic barrier to air masses moving from the Atlantic Ocean, which results in higher precipitation on the NW flank. The mean annual precipitation generally increases with the altitude up to 1900 mm in the highest areas (Niedźwiedź, 1992). The number of days with snow cover varies from 124 per year at the foothills to 228–236 days at 2000 m a.s.l. (Hess, 1996). The mean annual air temperature ranges from ~8 °C in the southern foothills to −3.7 °C at the top of Lomnický štít Mountain (2633 m a.s.l.). The climatic snow line at the southern slopes is located above the highest summits at ~2700–2800 m a.s.l., while it lies ~200 m lower on the northern slopes (Zasadni and Kłapyta, 2009).

The Velká Studená dolina (VS) and Malá Studená dolina (MS) valleys are located in the eastern part of the High Tatra Mts. SE from the main ridge. The valleys are incised into the southern part of the crystalline core consisting of biotite granodiorite-tonalite to muscovite-biotite granodiorite (Nemčok et al., 1994). Compound cirques surrounded by headwalls up to 400–500 m high form the upper part of the valleys above 1950–2000 m a.s.l. Extensive talus cones descend from the lower sections of the headwalls and cover most of cirque floors. A compound cirque in the VS Valley extends along a 3 km long section of the main ridge and belongs to one of the most extensive cirques in the range. The narrow Divá kotlina Cirque in the western part of the VS Valley head is separated by the prominent Svišťový chrbát hard rock ridge from the wide and less constrained cirque-in-cirque forms of the central and eastern part of the valley head (Fig. 2A). The MS valley head consists of two prominent cirques with their bottoms at ~2000 and 2190 m a.s.l. (Fig. 2B). Rock steps up to 400 m high represent the transition from compound cirques to troughs (Fig. 2C). The VS trough is 4 km long and it is significantly wider than the MS hanging trough which terminates ~150 m above the main trough (Fig. 2D). The pronounced glacial morphology of the troughs is modified by prominent gravity accumulations that cover the major part of the trough surfaces. The forefield of the VS trough is dominated by a complex topography of glacial deposits that are up to ~100 m thick. The morphologically pronounced moraines have been attributed to the last (Würmian) glaciation using morphological criteria and weathering characteristics of moraine boulders (Lukniš, 1973). However, this hypothesis has yet to be confirmed by numerical-age dating.

3. Methods

3.1. Sampling strategy

The overall sampling strategy was designed to identify and sample all relevant surfaces that could provide information about the local glaciation chronology. We sampled (1) boulders on the moraines, which best represent the timing of glacier advances and past climatic fluctuations (e.g., Gosse, 2005; Kerschner and Ivy-Ochs, 2008), (2) glacially-transformed bedrock surfaces, which indicate the timing and the rate of glacier retreat (e.g., Gosse et al., 1995; Briner et al., 2009), and (3) rockfall accumulations that have been formed as a direct consequence of deglaciation during the paraglacial period (*sensu* Ballantyne, 2002). We use the term rockfall accumulation for landforms resulting from free or bounding movement of rock fragments (Luckman, 2013).

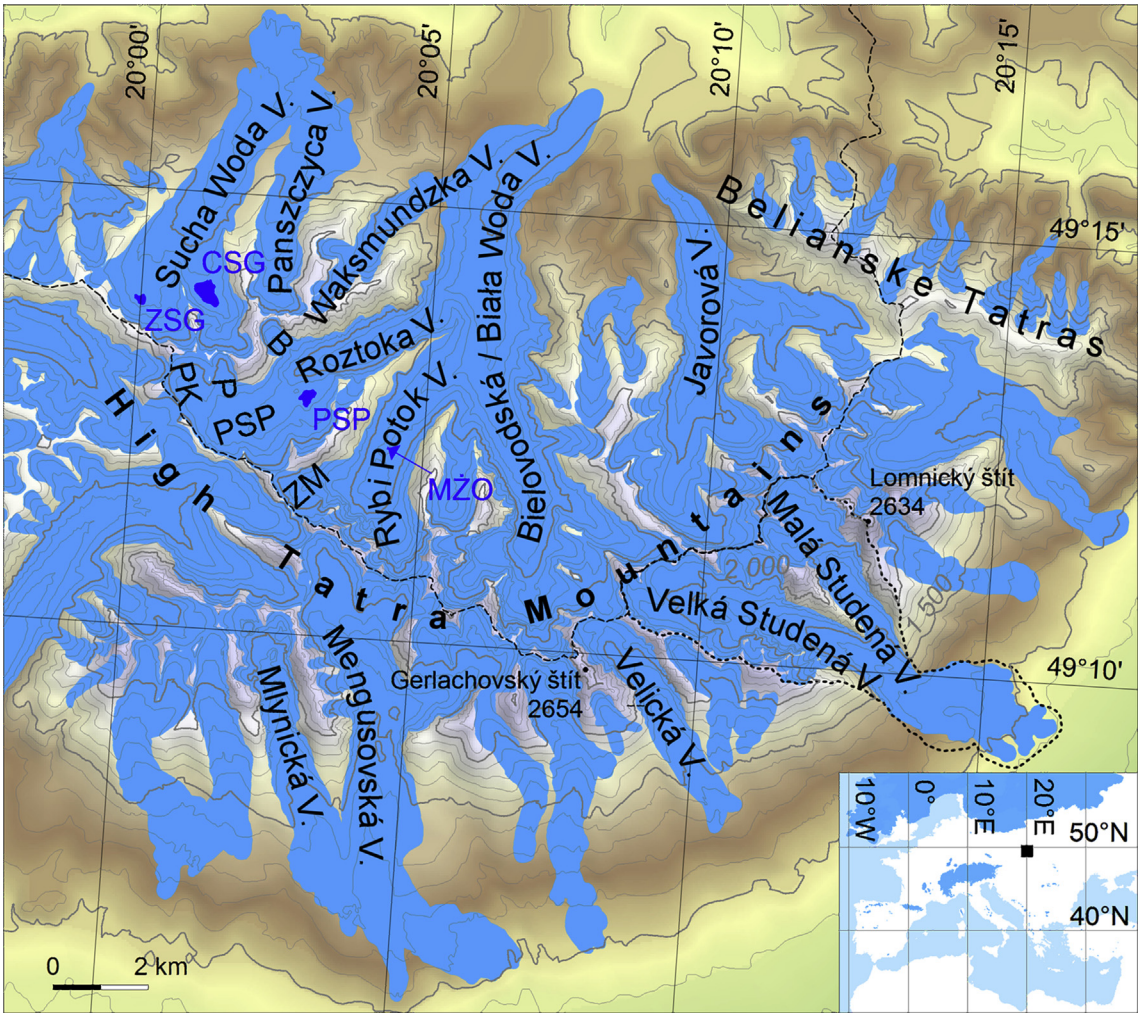

Fig. 1. Overview of the High Tatra Mts. and its position in Central Europe (inset). The LGM extent of glaciers (blue shades) in the High Tatra Mts. and Central Europe after Zasadni and Kłapyta (2014) and Ehlers et al. (2011), respectively. The valleys cited in the paper are indicated by full name or abbreviation (PK: Pod Kołem, P: Pusta, B: Buczynowa, PSP: Pięciu Stawów Polskich, ZM: Za Mnichem). Dark blue areas show the moraine-dammed lakes with dated sedimentary sequences (ZSG: Zielony Staw Gąsienicowy, CSG: Czarny Staw Gąsienicowy, PSP: Przedni Staw Polski, MŽO: Małe Żabie Oko) and a dashed line indicates the divide. A dotted line marks the location of the study area.

Surface exposure dating reflects a complete exposure history of morainic boulders, and the ages obtained may record an inheritance from an earlier exposure, post-glacial degradation and position changes of the boulder (e.g., Hallet and Putkonen, 1994; Ivy-Ochs and Kober, 2008). The selection of boulders for sampling is therefore an essential step in obtaining accurate ages. In order to achieve this, only large boulders situated on moraine crests have been sampled. Moreover, we sampled multiple boulders on the same moraine to minimise the impact of a sample with an anomalous exposure history (Gosse and Phillips, 2001). Following Putkonen and Swanson (2003), three boulders were sampled on small sharp-crested moraines and up to seven samples were collected on degraded moraine surfaces with gentle relief. A re-advance moraine below the mouth of the MS trough represents the only exception from our sampling rules as the lack of preserved boulders suitable for sampling precluded the collection of sufficient number of samples. Overall, 20 boulders were sampled on the moraines at the mouth of the VS trough (SD-01 to SD-03 and SD-05 to SD-15) and in the middle part of the MS trough (MSD-04 to MSD-06). In addition, three boulders (MSD-13 to MSD-15) were sampled on an ice-marginal fan close to the terminal moraine to constrain the timing of the initial glacier recession and the related moraine reworking. The sample site locations are shown in Fig. 3, and the site characteristics are given in Table 1.

Glacially polished bedrock surfaces were sampled to determine the timing of the glacier recession in those sections of the study area where alternative rock surfaces suitable for the dating of glacier retreat were not preserved. The samples were collected from surfaces formed by or significantly smoothed by glaciers to reduce the possibility of bedrock inheritance (e.g. Kelly et al., 2006; Ivy-Ochs and Kober, 2008; Dielforder and Hetzel, 2014). Only surfaces without vegetation, soil or debris cover were sampled to increase the probability of uninterrupted surface exposure since the time of deglaciation (Ivy-Ochs and Kober, 2008). Four samples were collected at the bottom of the troughs (SD-04, MSD-09, VSD-08 and VSD-09), three from the compound cirque steps (MSD-02, MSD-03, VSD-07) and three from the glacially polished rock steps that dam cirque lakes (MSD-01, VSD-05, VSD-06). In addition, four samples were collected at four different elevations on the Svišťový chrbát hard rock ridge that separates individual cirque-in-cirque forms of the VS valley (Figs. 3 and 4A). These bedrock samples (VSD-01 to VSD-04) are expected to give the timing and the rates of glacier thinning in the accumulation zone, provided that the glacier had the capacity to erode the rock ridge substantially.

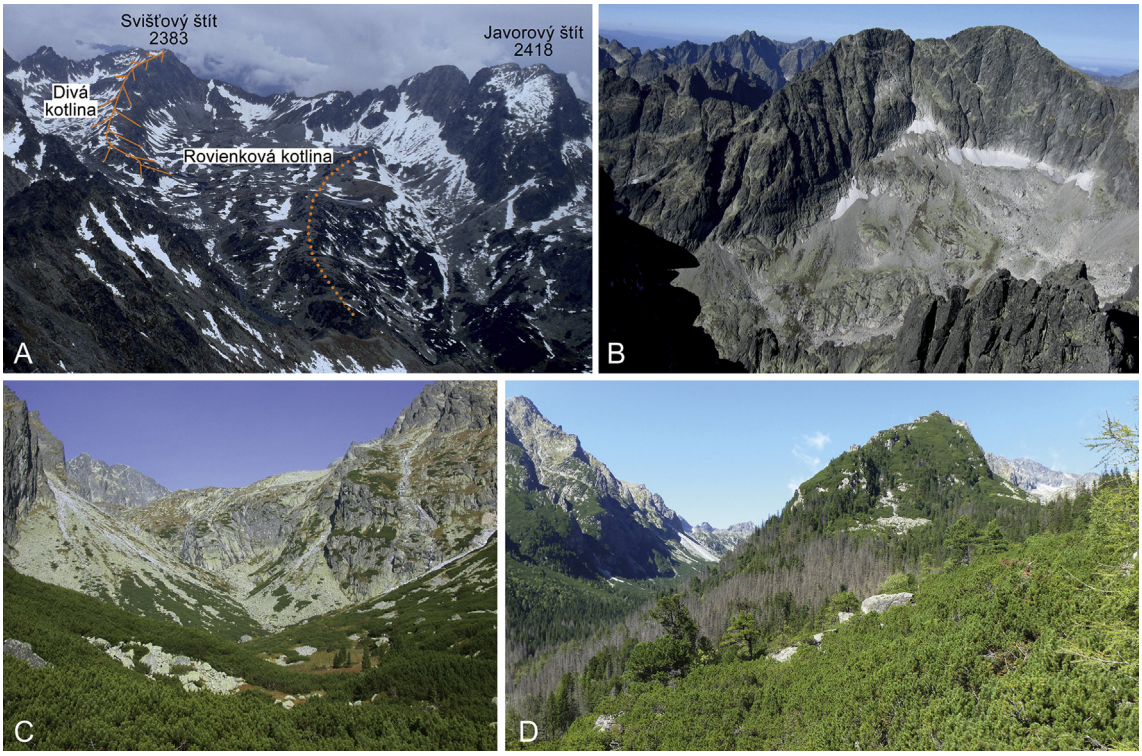

Fig. 2. (A) View of the Velká Studená dolina Valley head from SE. Full orange line shows sampled hard rock ridge and dotted line marks bedrock step between the cirque area and adjacent trough. Note contrast with the deep and narrow cirque in the Malá Studená dolina Valley seen from SE (B). (C) The backwall at the transition between the MS trough and adjacent cirque. (D) The junction of the MS (left) and VS (right) troughs.

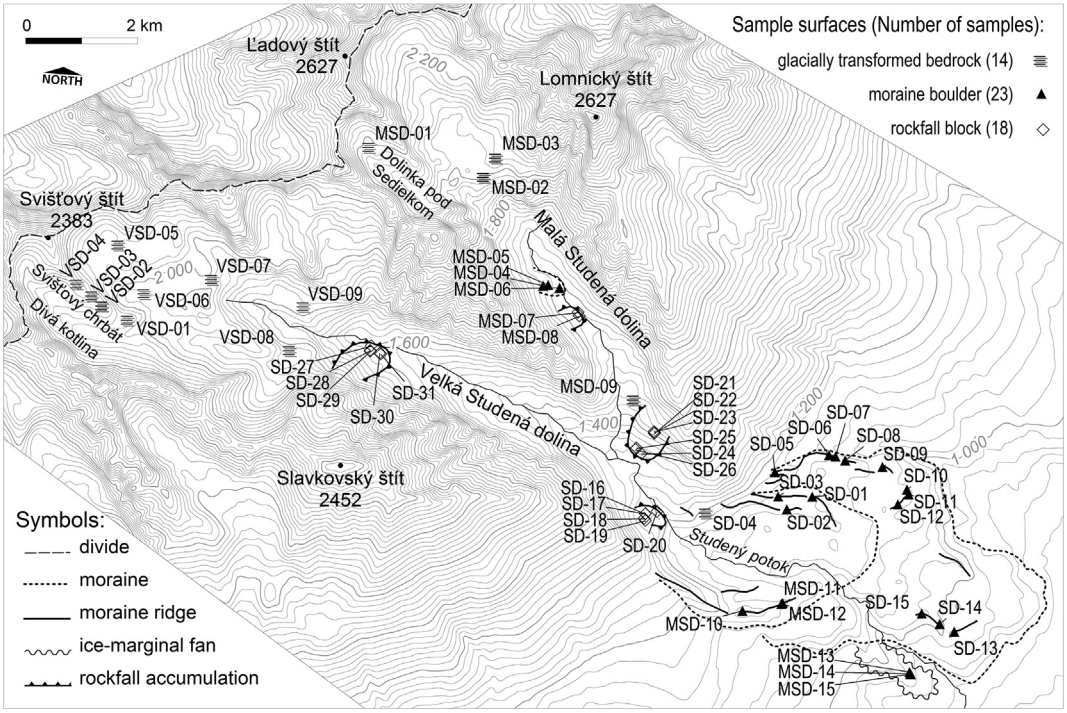

Fig. 3. Location of sample sites in the study area.

To constrain the timing of the glacier recession in the VS trough we sampled four rockfall accumulations that directly overlay the trough bottom or glacial accumulations. These accumulations are located at the distal end of the VS trough (SD-16 to SD-20), below the mouth of the MS (SD-21 to SD-26) and Varešková dolina hanging troughs (SD-27 to SD-31), and in the middle part of the MS trough (MSD-07 to MSD-08). The rockfall accumulation at the confluence of the VS and MS troughs covers the south-west-facing

Table 1
Sample sites characteristics and ^{10}Be surface exposure ages from the study area.

Sample	Altitude(m)	Boulder height (m)[a]	Surface dip/aspect (°)	Sample thickness (cm)	Topographic shielding factor	Snow cover depth/duration (cm/month)	Total shielding factor	Production rate ($at^{-1}\ g^{-1}\ yr^{-1}$)	^{10}Be concentration ($at^{-1}\ g^{-1}$)	^{10}Be uncertainty	^{10}Be age (yr)	Analytical uncertainty (±yr)	Total uncertainty (±yr)
MSD-01	2190	–	11/115	4	0.97122	64/7	0.90716	21.786	243,229	9495	11,153	435	804
MSD-02	1994	–	5/140	4	0.99516	59/7	0.93436	19.520	272,270	7979	13,939	409	939
MSD-03	2046	–	15/350	3	0.99252	60/7	0.93092	20.192	217,352	6418	10,749	317	725
MSD-04	1652	5.0	5/125	3	0.97960	49/6	0.93660	15.196	231,022	6922	15,186	455	1026
MSD-05	1634	1.5	Horizontal	4	0.98004	49/6	0.93702	15.000	237,285	8509	15,803	567	1113
MSD-06	1613	5.0	Horizontal	2	0.97627	48/6	0.93426	14.723	229,553	7207	15,574	489	1064
MSD-07	1580	3.5	Horizontal	4	0.97625	47/6	0.93508	14.366	229,452	9135	15,955	635	1157
MSD-08	1576	6.0	Horizontal	4	0.97731	47/6	0.93609	14.339	240,717	7208	16,772	502	1134
MSD-09	1469	–	5/10	4	0.99110	44/5	0.95839	13.518	205,333	6072	15,165	448	1022
MSD-10	1199	1.5	Horizontal	4	0.99946	36/5	0.97228	11.084	177,604	6285	15,989	566	1123
MSD-11	1160	3.0	10/110	4	0.99967	35/4	0.97850	10.808	156,099	5171	14,404	477	995
MSD-12	1160	2.0	Horizontal	3	0.99967	35/4	0.97850	10.810	126,273	4005	11,642	369	796
MSD-13	972	2.0	Horizontal	4	0.99933	30/4	0.98111	9.300	149,096	4369	15,984	468	1076
MSD-14	972	0.8	Horizontal	5	0.99972	30/4	0.98149	9.306	197,392	6705	21,176	719	1471
MSD-15	970	1.5	15/50	2	0.99949	30/4	0.98126	9.282	184,412	5462	19,828	587	1338
SD-01	1141	2.0	Horizontal	3	0.99897	35/4	0.97782	10.599	238,068	26,965	22,437	2541	2883
SD-02	1148	1.5	Horizontal	4	0.99902	35/4	0.97787	10.567	180,956	18,049	17,083	1704	1993
SD-03	1158	1.0	7/18	3	0.99875	35/4	0.97761	10.737	153,114	15,648	14,217	1453	1689
SD-04	1188	–	7/145	4	0.99693	36/5	0.96982	10.827	221,973	18,376	20,472	1695	2100
SD-05	1167	1.6	Horizontal	5	0.99815	35/5	0.97174	10.580	226,130	7199	21,344	680	1462
SD-06	1133	2.7	Horizontal	2	0.99860	34/4	0.97804	10.619	164,868	15,568	15,483	1462	1737
SD-07	1123	2.2	Horizontal	4	0.99839	34/4	0.97784	10.358	248,005	31,144	23,923	3004	3335
SD-08	1115	1.9	20/230	2	0.99741	34/4	0.97688	10.457	258,770	54,810	24,732	5238	5449
SD-09	1095	4.0	Horizontal	4	0.99932	33/4	0.97933	10.143	224,024	23,263	22,056	2290	2652
SD-10	1083	2.5	Horizontal	2	0.99953	33/4	0.97954	10.212	219,420	20,720	21,456	2026	2408
SD-11	1078	2.2	Horizontal	3	0.99953	33/4	0.97954	10.088	234,821	29,720	23,253	2943	3263
SD-12	1086	3.8	8/190	4	0.99953	33/4	0.97954	10.072	235,038	14,878	23,310	1476	2043
SD-13	999	1.3	Horizontal	6	0.99989	31/4	0.98107	9.243	200,452	12,660	21,644	1367	1894
SD-14	1007	2.1	Horizontal	3	0.99979	31/4	0.98097	9.534	268,423	43,664	28,150	4579	4887
SD-15	1032	1.2	5/310	1	0.99979	31/4	0.98097	9.896	171,945	26,614	17,329	2682	2841
SD-16	1227	4.5	4/230	2	0.98815	37/5	0.96055	11.241	257,713	23,538	22,910	2092	2512
SD-17	1231	2.0	6/170	2	0.98822	37/5	0.96062	11.278	207,025	21,485	18,322	1901	2202
SD-18	1246	1.3	Horizontal	5	0.98582	38/5	0.95757	11.098	264,821	39,176	23,848	3528	3813
SD-19	1242	5.1	5/250	3	0.98584	37/5	0.95831	11.261	131,259	13,702	11,615	1212	1402
SD-20	1223	1.7	22/70	4	0.99356	37/5	0.96582	11.082	199,729	27,039	17,987	2435	2668
SD-21	1382	5.5	15/180	5	0.98865	41/5	0.95817	12.359	219,028	33,505	17,692	2706	2911
SD-22	1406	4.4	14/180	6	0.98865	42/5	0.95746	12.486	204,994	32,506	16,385	2598	2782
SD-23	1409	6.0	Horizontal	2	0.98865	42/5	0.95746	12.938	210,065	13,896	16,206	1072	1454
SD-24	1312	4.7	19/150	2	0.99241	39/5	0.96325	12.061	211,518	23,910	17,506	1979	2245
SD-25	1312	5.6	15/185	3	0.99259	39/5	0.96343	11.966	210,288	23,794	17,543	1985	2252
SD-26	1307	4.3	horizontal	2	0.99206	39/5	0.96291	12.011	233,506	31,056	19,415	2582	2838
SD-27	1613	4.1	11/42	6	0.98109	48/6	0.93887	14.356	214,047	22,227	14,882	1545	1790
SD-28	1618	5.1	Horizontal	4	0.98196	48/6	0.93970	14.663	197,823	33,141	13,463	2255	2399
SD-29	1636	3.8	Horizontal	5	0.98203	49/6	0.93893	14.721	210,691	24,380	14,285	1653	1866
SD-30	1622	4.2	12/295	3	0.98194	48/6	0.93968	14.823	242,428	15,346	16,333	1034	1432
SD-31	1622	4.1	13/312	3	0.98194	48/6	0.93968	14.823	271,868	35,367	18,325	2384	2630
VSD-01	2077	–	4/155	5	0.99540	61/7	0.93264	20.558	313,733	10,431	15,258	507	1055
VSD-02	2138	–	Horizontal	3	0.99849	63/7	0.93359	21.486	342,904	10,756	15,961	501	1090
VSD-03	2154	1.4	15/130	4	0.99801	63/7	0.93315	21.720	353,159	12,014	16,263	553	1131
VSD-04	2216	–	7/20	5	0.99918	65/7	0.93230	22.657	400,565	13,397	17,691	592	1225
VSD-05	2075	–	Horizontal	3	0.99372	61/7	0.93107	20.497	305,471	9493	14,899	463	1015

VSD-06	1974	–	Horizontal	4	0.99452	58/6	0.94328	19.319	299,077	9317	15,476	482	1055
VSD-07	1998	–	Horizontal	3	0.99698	59/7	0.93608	19.499	366,467	11,427	18,804	586	1282
VSD-08	1841	–	Horizontal	4	0.99300	54/6	0.94519	17.571	276,926	8909	15,752	507	1081
VSD-09	1822	–	Horizontal	4	0.99248	54/6	0.94470	17.316	281,037	9020	16,222	521	1113

[a] Blank field marks bedrock site.

side of the VS trough, and the three other accumulations are located on the north-east-facing slopes of the trough. The samples from these accumulations should provide an age of paraglacial rockfall events indicating a minimum age estimate of the initial glacier retreat in the trough. In order to increase the accuracy of the resulting chronology, five to six blocks were sampled on each rockfall accumulation (except for the accumulation in the MS trough where only two boulders were sampled). While dating multiple samples does not guarantee that the timing reconstructed is correct, it increases the probability that the oldest age will coincide with the landform's age (Zreda and Phillips, 1995). The samples have been collected from the blocks located on the terminal section of the rockfall accumulations to reduce the possibility of sampling a single block that fell later than during the main event (Delunel et al., 2010).

The samples were collected preferentially from boulders larger than 1 m. This was aimed to reduce the possibility of post-depositional exhumation of boulders and to avoid the effects of snow and vegetation cover. Only horizontal to slightly dipping top surfaces of the boulders were sampled at the centre to minimise edge effects (Gosse and Phillips, 2001) and the effects of neutron loss (Masarik and Weiler, 2003). The samples were collected using a chisel and a hammer to the depth of 2–5 cm. The dip and orientation of the sampled surfaces were measured with a clinometer and a compass. The geometry of the surrounding topography was recorded using a digital camera with fish-eye lens, and the location and altitude of the sample sites were determined with GPS. All the sampled surfaces were composed of medium-grained to coarse-grained biotite monzogranite. Overall, 41 samples were collected from the boulders on the glacial (23 boulders) and slope (18 blocks) accumulations and 14 samples were collected from bedrock surfaces.

A Schmidt hammer (SH) was used to derive rebound (R) values for the sampled surfaces to allow an approximate correlation of the moraines in the range and the identification of individual boulders that are affected by inheritance. Inheritance could be indicated by a discrepancy between the measured R-values and exposure ages, or by apparently higher ages compared with the adjacent moraines (Engel et al., 2014). The mean R-value of each moraine was calculated based on 150 SH measurements undertaken on boulders. Horizontal surfaces of six boulders were measured with a SH, each with 25 impacts, following Moon's (1984) guidelines. The mean R-values from the six boulders were averaged and the resulting value was taken as representative for a given moraine. Analysis of variance was used to determine if any differences exist in the mean R-value among the groups of moraines. The significance of the relationship was tested by the F test with p-level of 0.05.

3.2. Sample preparation and data treatment

The granite samples were crushed, sieved and cleaned with a mixture of HCl and H_2SiF_6. The extraction method for ^{10}Be ($T_{1/2} = 1.387 \pm 0.012$ Ma; Korschinek et al., 2010; Chmeleff et al., 2010) involves the isolation and purification of quartz and the elimination of atmospheric ^{10}Be. A weighed amount (~0.1 g) of a 3025 ppm solution of ^{9}Be was added to the decontaminated quartz. Beryllium was subsequently separated from the solution by successive anionic and cationic resin extraction and precipitation. The final precipitates were dried and heated at 800 °C to obtain BeO and finally mixed with niobium powder prior to the measurements, which were performed at the French Accelerator Mass Spectrometry (AMS) National Facility. The beryllium data were calibrated directly against the National Institute of Standards and Technology beryllium standard reference material 4325 using an assigned value of $(2.79 \pm 0.03) \cdot 10^{-11}$. Age uncertainties include AMS internal

Fig. 4. (A) Ice-scoured slabs on the Sviščový chrbát hard rock ridge at 2077 m, location of the sample VSD-01. (B) Lateglacial moraine in the Rovienková kotlina Cirque between the sample sites VSD-05 and VSD-06.

variability (<0.5%), an external AMS uncertainty of 0.5% (Arnold et al., 2010), blank correction and 1σ uncertainties. Long-term measurements of chemically processed blanks yield ratios in the order of $(3.0 \pm 1.5)\cdot 10^{-15}$ for ^{10}Be. A sea-level, high-latitude spallation production of 4.03 ± 0.18 at $g^{-1}\cdot yr^{-1}$ was used and scaled for latitude (Stone, 2000) and elevation. This production rate is a weighted mean of recently calibrated production rates in the Northern Hemisphere: North-eastern North America (Balco et al., 2009), Northern Norway (Fenton et al., 2011), Southern Norway (Goehring et al., 2012) and Greenland (Briner et al., 2012). All the individual production rates have been corrected relative to a ^{10}Be half-life of 1.387 Ma. Cosmic Rays Exposure ages were calculated using the equation described by Braucher et al. (2013).

The surface production rates were also corrected for the local slope and topographic shielding due to the surrounding terrain following Dunne et al. (1999). Shielding from snow was estimated according to Gosse and Phillips (2001) using an average snow density of 0.3 g cm^{-3}, the mean depth and duration of snow cover in the study area. These values were estimated from data collected during the years 1960/61–1989/90 at five weather stations (827–2635 m a.s.l.) in the range (Kočický, 1996). As the snow cover is unevenly distributed and its variation since the exposure of sampled surfaces is unknown, the real effect of snow shielding remains uncertain. However, most of samples were extracted from windswept sites without vegetation and we therefore suspect that temporal variation in snowfall has had a minor effect on snow conditions at these sites.

3.3. Exposure age interpretation

Cosmogenic exposure dating is a powerful method for reconstructions of Quaternary glaciation histories of mountain regions (Balco, 2011). A multi sample approach has been frequently applied on moraines and mass movement accumulations to increase the accuracy and reliability of the obtained exposure data (e.g. Gosse and Phillips, 2001; Rinterknecht et al., 2006; Briner, 2009). However, multi exposure data have been treated in different ways, which may result in contrasting exposure age interpretations. In some studies, the exposure age of the oldest boulder was interpreted as best reflecting the deposition age of the sampled moraine (e.g., Zreda et al., 1994; Putkonen and Swanson, 2003; Briner et al., 2005). Alternatively, the error-weighted mean (e.g., Tschudi et al., 2000; Briner et al., 2001) and the arithmetic mean (e.g., Ivy-Ochs et al., 2007) of all ages were preferred when age distributions overlap within a 1-σ uncertainty. If the comparison of exposure data from a single accumulation reveals unreasonably low or high ages, outliers should be excluded from the treated dataset. Unfortunately, there is no generally accepted procedure to identify and remove outliers from multiple sample datasets. In cases where there are at least three ages, several statistical criteria may be used. The chi-square test (e.g. Ward and Wilson, 1978), Chauvenet's criterion (Rinterknecht et al., 2006) and Peirce's criterion (Dyke et al., 2014) are the most commonly applied procedures in dating applications.

In this study, we applied the method proposed by Dunai (2010) to multiple exposure ages (n) from our sampled accumulations. The distribution of exposure ages obtained from a given accumulation was examined, and the ages of boulders affected by inheritance (apparently old ages) or post-depositional changes (young ages) were identified as outliers. The outliers were excluded from the sample (age) population of a given accumulation using chi-square (χ^2) analysis. A 95% critical value for χ^2 with n-1 degrees of freedom was calculated and compared with the theoretical value. If the calculated value was lower than the theoretical one, all ages were used to calculate the mean exposure age. Alternatively, outliers were excluded from further consideration until the distribution passed the χ^2 test. The arithmetic mean exposure age and the error-weighted mean exposure age with associated analytical uncertainties were calculated from the final dataset and taken as representative for the moraine. Exposure ages with a 1σ uncertainty are reported in the ^{10}Be time scale.

Analytical uncertainties were taken into account when the mean exposure ages were compared with the remaining exposure ages from the sample sites. The mean exposure ages with related uncertainties were interpreted as representing the timing of deposition of all but two of the sampled moraines and slope accumulations. In these cases, we took into account that the mean exposure age of boulders differs from the timing of moraine deposition and age distributions tend to tail to a younger age (Phillips et al., 1990; Zreda and Phillips, 1995). Consequently, the oldest exposure ages obtained for these accumulations were interpreted to represent the timing of deposition. The set of the obtained exposure ages was used to establish a local glaciation chronology following general interpretation strategies (Ivy-Ochs et al., 2007; Phillips et al., 1990). Exposure ages from rockfall accumulations were used to constrain the deglaciation chronology and their detailed interpretation is a subject to another paper. Moreover, ^{10}Be ages from the bedrock samples were used to quantify the rates of glacier decay. ^{10}Be ages obtained for trough and cirque floor sites allowed for the determination of rates of glacier termini retreat (e.g. Briner et al., 2009) whereas the ages from the elevation transect were used to quantify the rates of glacier thinning (e.g. Stone et al., 2003). The established glacial chronology and glacier retreat rates were subsequently compared

with previously published chronological data from the High Tatra Mts. and other relevant sites in central Europe. For these comparisons, 6% maximum uncertainty associated with the production rate and 1% uncertainty associated with the half-life estimation have been added to the analytical uncertainties (Stone, 2000).

3.4. GIS analysis and modelling

Digital elevation models (DEMs) of former glaciers were generated following the procedure described by Mentlík et al. (2013). The models were used to calculate the glacier area, the volume and the ELA for the glaciation phases identified in the study area. The reconstruction of glacier extent was based on the delimitation of moraine ridges and glacially polished bedrock surfaces. The topography of landforms identified in the field was extracted from the existing 15 m grid DEM produced by digital photogrammetry from aerial photographs. Due to the absence of moraines in the upper part of the both valleys, the approximate extent of the youngest phase was inferred from dated bedrock surfaces. The upper headwall limit of ice was estimated by extrapolating the ice surface from geomorphological evidence to a point on the backwall cliff (Hughes, 2010). The surfaces of former glaciers were contoured by extrapolating from points at the suggested ice margins. Ice surface contours were drawn as concave in the upper part, convex in the lower part and straight in the middle parts of the former glaciers (Carr and Coleman, 2007). The modelled glacier surfaces were superimposed over the current topography and the approximate ice volume for glaciation phases was calculated neglecting the postglacial valley infill. The relevant ELAs were calculated using the accumulation area ratio (AAR) and steady-state AAR (ssAAR$_0$) methods (e.g. Benn et al., 2005; Kern and László, 2010; Makos et al., 2014).

4. Results

4.1. Moraines and rockfall accumulations

All but one exposure ages obtained for the boulders on the terminal moraine and related left lateral moraines are consistent. Seven samples collected from the terminal moraine have a mean exposure age of 22.0 ± 0.8 ka (Fig. 5 and Table 2). One sample (SD-06) from the adjoining lateral moraine was identified and rejected as an outlier on the basis of the χ^2 analysis. Three other samples yield a mean exposure age of 21.5 ± 0.7 ka. Altogether, ten samples from the oldest preserved moraine yield a mean exposure age of 21.7 ± 0.5 ka. Out of the three samples extracted from the ice-marginal fan in front of the terminal moraine, one (MSD-13) was rejected as an outlier. The remaining two samples yield a mean exposure age of 20.4 ± 0.5 ka.

A prominent group of re-advance moraines at the mouth of the VS trough is represented by six boulder samples. However, the exposure ages obtained for these boulders reveal considerable scatter, ranging from 22.4 ± 2.5 to 11.6 ± 0.4 ka (Table 1). Out of the three samples extracted from the double-ridged moraine surface on the left side of the Studený potok Brook (Fig. 5), the youngest one (SD-06) was excluded from further consideration based on the results of the χ^2 test. The other two samples yield a mean exposure age of 18.7 ± 1.4 ka. Three exposure ages obtained for a more pronounced moraine on the right side of the brook have a scattered pattern which precludes the selection of two overlapping ages. The most deviating age of 11.6 ± 0.4 ka (MSD-12) was removed from the dataset using the χ^2 analysis however the other two samples also failed the test. The older of these samples (MSD-10) was subsequently considered together with samples SD-1 and SD-2 from the double-ridged moraine but it appears to be an outlier. Therefore, the final data set for the re-advance moraines at the mouth of the VS trough consists of only two samples. Possible reasons for inconsistent exposure ages are discussed in the Section 5.1. The exposure ages obtained for the boulders on the re-advance moraine in the MS trough are consistent and yield a mean exposure age of 15.5 ± 0.3 ka.

Out of the 18 exposure ages obtained for the boulders on rockfall accumulations, only one was rejected as an outlier on the basis of the χ^2 test. The outlying age was obtained for sample SD-19 on the surface of the lowermost sampled rockfall accumulation (Table 2). The remaining four samples collected on this accumulation yield a mean exposure age of 20.2 ± 1.2 ka. Six samples from the accumulation below the mouth of the MS yield a mean exposure age of 17.0 ± 0.7 ka and five samples collected below the Varešková dolina hanging trough give a mean exposure age of 15.6 ± 0.7 ka. The small accumulation in the MS trough has a mean exposure age of 16.5 ± 0.4 ka.

The variability of the R-values measured on the moraines and rockfall accumulations is low (Table 2). A mean R-value of 38.5 ± 4.5 obtained for the terminal moraine overlaps within the standard deviation with the mean R-values calculated for the ice-marginal fan (36.0 ± 5.7) and re-advance moraines (34.6 ± 4.5 to 39.0 ± 6.8). Among the moraine belts and rockfall accumulations (34.5 ± 4.5 to 41.4 ± 5.6), there are no significant differences in the mean R-values either. The absence of significant differences may be attributed to the relatively short interval (~22–15.5 ka) from which the sampled landforms originate. The low variability of Schmidt hammer data from different accumulations also suggests that the effects of post-exposure erosion and weathering on the sample surfaces are negligible.

4.2. Bedrock surfaces

Fourteen samples extracted from the trough bottom, cirque floor and the hard-rock ridge in the accumulation zone of a former VS glacier gave surface exposure ages ranging from 20.5 ± 1.7 ka to 10.7 ± 0.3 ka. All the ages are consistent with the geomorphological position of the sampled bedrock surfaces, increasing from the lower section of troughs to cirques or decreasing with the elevation of the Svišťový chrbát hard rock ridge (Figs. 5 and 6). The distribution of the exposure ages (Fig. 7) indicates three populations of glacially transformed surfaces that may represent the intervals of local glacier recession discussed in Section 5.1.

The exposure ages obtained for glacially modified bedrock surfaces in the VS valley range from 20.5 ± 1.7 ka in the lower part of the trough to 14.9 ± 0.5 ka in the largest cirque located on the valley axis (Fig. 5). The succession of the exposure ages represents a consistent record of a glacier retreat from the trough. The ^{10}Be age of 18.8 ± 0.6 ka obtained for the sample VSD-07 indicates the timing of the emergence of the dividing ridge between the main cirque and the erosional extension of the trough towards the northernmost cirque-in-cirque form (Figs. 2A and 3). The exposure ages obtained from the Svišťový chrbát hard rock ridge decrease consistently from the upper section of the ridge (17.7 ± 0.6 ka) to its lower part (15.3 ± 0.5 ka) providing an exceptional opportunity to establish a glacier thinning rate in the cirque (see the Section 5.2.).

The exposure ages from the bottom of the MS hanging valley decrease with the increasing elevation from 15.2 ± 0.4 ka to 11.2 ± 0.4 ka. These ages were obtained for surfaces with clear evidence of glacial erosion (polished rock with grooves), which are located far from the surrounding blockfields. The only sample collected from a lateral position above the MS valley floor (MSD-03) yields an age of 10.7 ± 0.3 ka, which is lower than the age of 13.9 ± 0.4 ka obtained for the lowermost site (MSD-02) on the cirque step. The lower age for the MSD-03 sample is consistent with

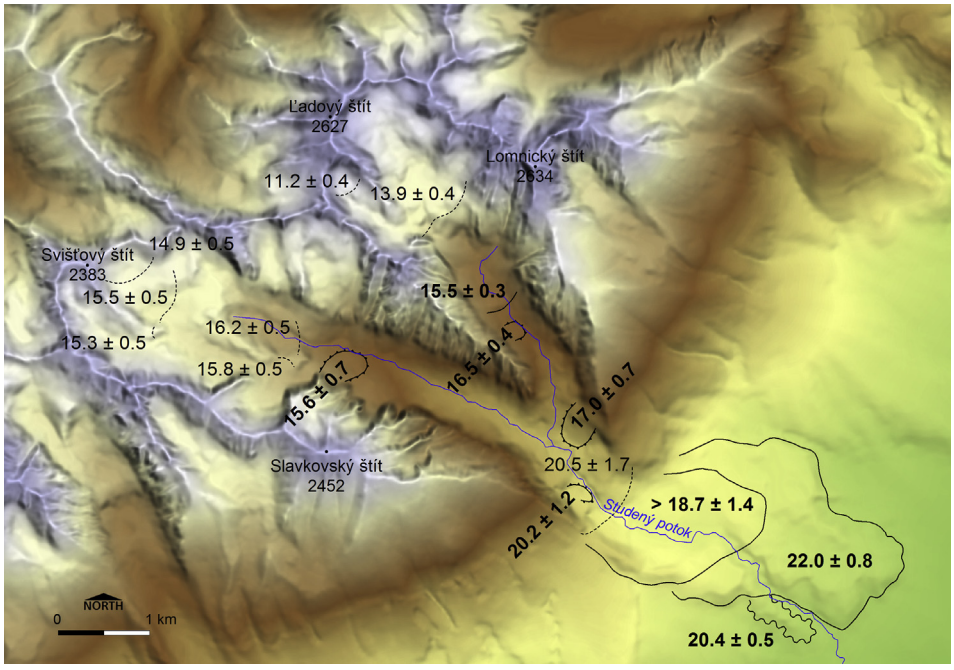

Fig. 5. ^{10}Be exposure ages for bedrock surfaces and weighted mean ages (in bold) for moraines and rock-falls in the study area. Full lines indicate outer limit of moraines, lines with triangles show rock-fall accumulations and dashed lines mark the deglaciation chronology.

later deglaciation of the upper part of the cirque step but the age difference between the two sites appears too large. Possible explanations are presented in Section 5.1.

5. Interpretation and discussion

5.1. Glaciation chronology in the study area

The exposure ages obtained for the terminal moraine in the forefield of the VS valley indicate that the oldest preserved moraine ridges represent the global LGM in Marine Isotope Stage (MIS) 2 (e.g. Hughes et al., 2013). Both the arithmetic and error-weighted mean exposure ages of 22.5 ± 2.6 ka and 22.0 ± 0.8 ka, respectively, suggest that the VS glacier reached its maximum extent close to the peak of the last glacial period (Table 2). Even the oldest age of 28.2 ± 4.6 ka from the terminal moraine falls within the interval between the onset of the expansion of ice sheets and their maximum extent (Clark et al., 2009). This view contradicts the chronology proposed by Lukniš (1964) which matches the greatest glacier extent below the VS valley with the Middle Würmian glaciation (MIS 4). However, this assumption was based on morphologic criteria and relative-age indicators, which provide very rough age estimates.

The arithmetic mean age of 22.5 ± 2.9 ka calculated for the terminal moraine below the VS valley correlates (within total uncertainties of exposure data) with the mean ^{36}Cl exposure ages

Table 2
^{10}Be surface exposure ages and the mean Schmit hammer R-values from moraines and rockfall accumulations (RA) in the VS and MS Valleys.

Phase	Landform	Minimum altitude (m a.s.l.)	R-value	Number of samples/ sample code	Critical χ^2	95% χ^2	Weighted mean age ± analytical uncertainty (yr)	Arithmetic mean age ± analytical uncertainty (yr)	Arithmetic mean age ± total uncertainty (kyr)	Maximum age ± analytical uncertainty (kyr)
LGM	Terminal moraine	870	38.5 ± 4.5	7/SD-09 to SD-15	12.59	5.94	22,045 ± 760	22,457 ± 2604	22.5 ± 2.9	28.2 ± 4.6
	Lateral moraine	1090	41.6 ± 3.7	4/SD-05 to SD-08	7.81	15.27				
				3/SD-05, SD-07, SD-08	5.99	1.08	21,521 ± 658	23,333 ± 3345	23.3 ± 3.6	24.7 ± 5.2
	Ice-marginal fan	920	36.0 ± 5.7	3/MSD-13 to MSD-15	5.99	47.23				
				2/MSD-14, MSD-15	3.84	2.11	20,367 ± 455	20,502 ± 653	20.5 ± 1.4	21.2 ± 0.7
Re-advance	Left lateral moraine	1080	34.6 ± 4.5	3/SD-01 to SD-03	5.99	8.04				
				2/SD-01, SD-02	3.84	3.06	18,744 ± 1415	19,760 ± 2109	19.8 ± 2.4	22.4 ± 2.5
	Right lateral moraine	1100	38.2 ± 5.1	3/MSD-10 to MSD-12	5.99	48.04				
				2/MSD-10, MSD-11[a]	3.84	4.59				
				1/MSD-10	–	–				16.0 ± 0.6
Deglaciation	RA at the VSD mouth	1220	41.4 ± 5.6	5/SD 16 to SD-20	9.49	31.08				
				4/SD-19 excluded	7.81	4.55	20,226 ± 1151	20,767 ± 2529	20.8 ± 2.8	23.8 ± 3.5
	RA at the MSD mouth	1290	38.1 ± 6.2	6/SD-21 to SD-26	11.07	1.68	16,968 ± 742	17,458 ± 2210	17.5 ± 2.5	19.4 ± 2.6
	RA in the VSD trough	1590	40.9 ± 8.0	5/SD-27 to SD-31	9.49	3.56	15,582 ± 691	15,458 ± 1870	15.5 ± 2.1	18.3 ± 2.4
	RA in the MSD trough	1570	34.5 ± 4.5[b]	2/MSD-07, MSD-08	3.84	1.02	16,458 ± 394	16,364 ± 576	16.4 ± 1.1	16.8 ± 0.5
	Re-advance moraine	1610	39.0 ± 6.8	3/MSD-04 to MSD-06	5.99	0.78	15,478 ± 287	15,521 ± 505	15.5 ± 1.1	15.8 ± 0.6

[a] The sample excluded based on comparison with ages of adjacent moraines.
[b] The mean of two values only.

reported by Makos et al. (2014) for the terminal moraines in the Velická (24.7 ± 1.4 ka) and Sucha Woda (20.1 ± 1.1 ka) valleys (Figs. 1 and 9). These figures confirm the view that all the moraines preserved in the range were formed during the last glacial period (Dzierżek, 2009) and that the largest expansion of glaciers occurred no later than 21.5 ka (Makos et al., 2013a). Similar conclusions have recently been reported from the Bavarian Forest (Reuther et al., 2011) and the Krkonoše Mts. (Engel et al., 2011), located 500 and 350 km W of the study area, respectively (Fig. 10). A larger expansion of local glaciers during MIS 2 than in earlier phases of the last glacial period is also in accordance with the evolution of glaciations in the Alps (van Husen, 2011) and the Southern Carpathians (Ruszkiczay-Rüdiger et al., 2014). In the Rodna Mts. (Eastern Carpathians), located 400 km ESE of the study area (Fig. 10), the most extensive glacial advance occurred within the last glacial period, but before ca. 37 ka (Gheorghiu et al., 2011). The LGM ELA at 1640 m a.s.l. calculated for VS and MS glaciers (Table 3) is in accordance with the ELA values reported by Makos et al. (2014) for the Mlynická (1650 m a.s.l. AAR 0.65) and Velická (1700 m a.s.l. AAR 0.63) glaciers on the southern flank of the range. At the same time, the ELA was ~180 m lower in the north-facing valleys of Sucha Woda and Pańszczyca (Makos et al., 2014).

The initial retreat of the VS glacier from its LGM position remains undated. However, the exposure ages obtained for the ice-marginal fan suggest that the western margin of the latero-frontal moraine was breached around 20.4 ± 0.5 ka. This moraine section might have been reworked at the time of the post-LGM glacier recession or even later during the subsequent glacier re-advance/recession. Because the first re-advance terminated no later than 20.5 ± 1.7 ka, the initial post-LGM retreat must have occurred well before ~21 ka. This inference is in agreement with the tentatively suggested onset of the post LGM deglaciation in the range around 21.5 ka (Makos et al., 2013a). Moreover, by around 21 ka the Alpine glaciers had started to retreat from their maximum position (Preusser, 2004; Ivy-Ochs et al., 2004; Pellegrini et al., 2005; Preusser et al., 2011).

The first re-advance of the VS glacier after the local LGM occurred before about 20.5 ka. This re-advance resulted in the deposition of lateral moraines near the mouth of the VS trough around 1.4 km up-valley from the terminal moraine (Fig. 5). The exposure age of 20.5 ± 1.7 ka has to be considered a minimum for the moraine deposition because it indicates a subsequent glacier retreat from the bedrock surface (SD-04) behind the moraine. This

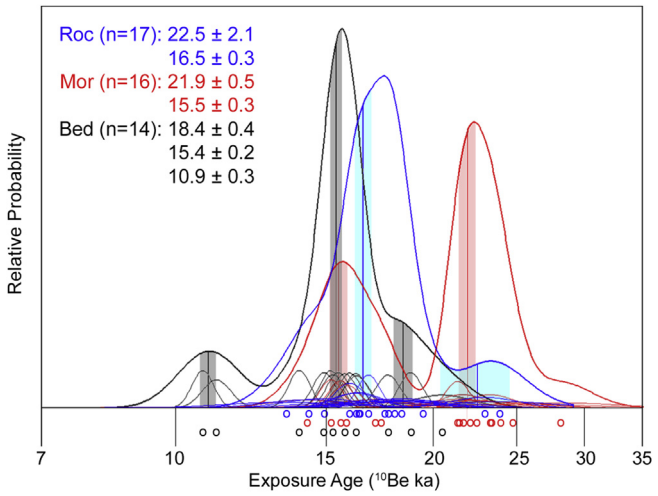

Fig. 7. The probability distribution of ^{10}Be exposure age obtained for rockfall accumulations (blue), moraines (red) and bedrock surfaces (black). Open circles and coloured lines show individual exposure ages with analytical uncertainties. Thick lines mark Kernel Density Estimation and vertical lines with shading indicate mean ages with proportions for modelled peaks (Vermeesch, 2012). Data are presented on a logarithmic scale.

interpretation is supported by the exposure age and the position of a rockfall accumulation close to the bedrock site showing that this section of the valley was ice free around 20.2 ± 1.2 ka. By contrast, the exposure data from individual moraine boulders show predominantly lower ages and considerable scatter (Table 2). A comparison of the ages obtained for the moraine boulders, the bedrock site and the rockfall accumulation suggests that the boulder exposure ages are mostly younger than the true age of deposition. Only two boulder ages that passed the χ^2 test yield mean ages that overlap within the uncertainties of ^{10}Be ages for the above-mentioned bedrock site. The maximum age obtained from the recessional moraine (22.4 ± 2.5 ka) is in accordance with the maximum ages from the terminal and related recessional moraines and with the exposure ages for the apparently younger bedrock and rockfall accumulation above the moraine. The second exposure age (17.1 ± 1.7 ka) from the reduced dataset represents a small inner ridge of the double-ridged left lateral moraine. According to the

Fig. 6. Location of sample sites on the Svišťový chrbát hard rock ridge and reconstructed glacier surfaces corresponding to each site.

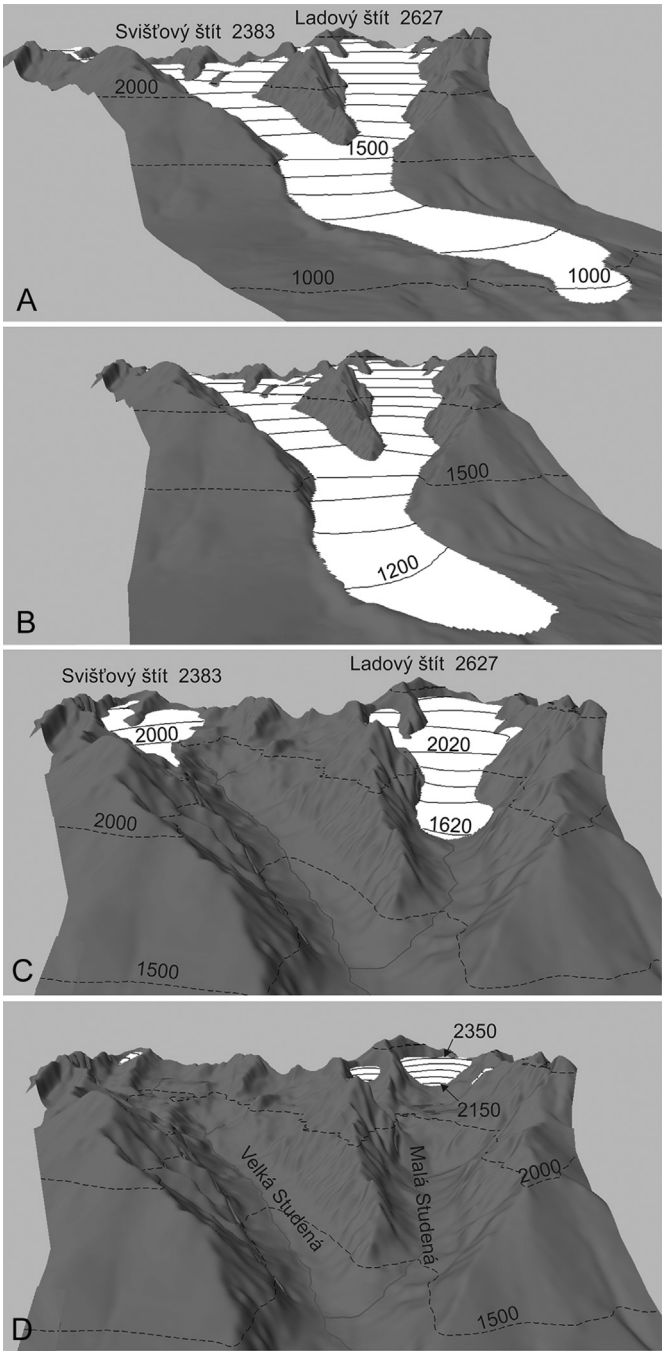

Fig. 8. Reconstruction of the VS and MS glaciers during the LGM (A), around 20.5 ka (B), 15.5 ka (C) and 12 ka (D). All views from SE. No vertical exaggeration.

morphology of moraines and the available exposure ages, the first post-LGM advance was followed by a glacier retreat from the recessional moraine and a subsequent re-advance that terminated close to the previous advance.

A large scatter of the boulder exposure ages can be partly explained by the lack of moraine boulders available for sampling. The number of upright boulders embedded in the moraine crests is limited on the right lateral moraine and even more restricted on the opposite moraine where surface degradation is also more significant. The lower exposure ages from these relics may be attributed to the post-depositional thawing of dead ice, frost-heave and related movements of the sampled boulders (e.g. Putkonen and Swanson, 2003; Ivy-Ochs et al., 2007). The effect of position changes, burial by glacial sediments or dead ice was recently considered as a potential reason for the lower than expected exposure ages for a similar moraine in the Mlynická Valley (Makos et al., 2014). The reasons for the scattered and considerably low exposure ages from the right lateral moraine in the study area are not known. The well-preserved morphology of this moraine and significantly fewer indices of its surface degradation suggest that burial and subsequent exhumation of moraine boulders is not probable. However, post-depositional surface weathering, rotation or toppling of the boulders cannot be excluded as well as the effects of vegetation and snow cover shielding (e.g. Favilli et al., 2009; Balco, 2011; Heyman et al., 2011).

The first re-advance (>20.5 ka) of the glaciers in the study area after the maximum LGM advance overlaps with the formation of the "inner" terminal moraine in the Sucha Woda Valley, where six exposure ages range from 20.9 to 16.7 ka (Makos et al., 2014). Within the total uncertainties, the age of 20.5 ± 2.1 ka also coincides with the exposure ages reported by Makos et al. (2014) from lateral moraines in the Velická (22.8–19.5 ka) and Mlynická (19.6–17.8 ka) valleys (Fig. 9). However, these moraines were related to the maximum extent of the glacier and the reported ages were considered as too young (Makos et al., 2014). The timing of the initial post-LGM glacier re-advance prior to 20.5 ka in the study area is broadly synchronous with the younger LGM glacier expansion in the Alps (~21 ka; e.g. Starnberger et al., 2011; van Husen, 2011) and the Bavarian/Bohemian Forest (~22 ka; Mentlík et al., 2013). It is also consistent with the two-fold glacier advances during the global LGM interval in the Krkonoše Mts. (Engel et al., 2014). Chronological indices for equivalent glacier expansion have not been reported from the Carpathians apart from the High Tatra Mts.

The exposure age of 20.5 ± 1.7 ka from the bedrock site at the mouth of the VS trough represents the earliest evidence of glacier recession after the first post-LGM re-advance. The exposure of the sample site indicates a retreat of the glacier terminus from the forefield of the VS valley into the trough. The initial phase of the recession is also constrained by the exposure ages from the bedrock sites in the upper part of the valley. The exposure age of 18.8 ± 0.6 ka obtained from a hard rock divide in the eastern part of the cirque documents a downwasting in the accumulation zone of the glacier. The thinning of the glacier due to the melting led to the emergence of the dividing bedrock ridge and a subsequent disintegration of the glacier to individual lobes from cirque-in-cirque forms (Fig. 8B). As a result, the ice flow from the main cirque over the rock barrier eastward was reduced and eventually ceased. The main glacier flow was restricted to the right side of the valley that joins the VS trough as a hanging valley. The lobes from the northern section of the compound cirque were confined to the left side of the trough. The timing of an overall glacier recession after ~20 ka supports the hypothesis of a prolonged period of post-LGM climate warming and related deglaciation in the range that lasted until 18–17 ka (Makos et al., 2013a). The retreat of the glaciers in the study area is also in accordance with the phase of the early Late-glacial ice decay in the Alps that was reported from both the Alpine foreland and inner valleys (e.g. Reitner, 2007; Dielforder and Hetzel, 2014).

Post-LGM glacier retreat was interrupted by a glacier re-advance no later than 15.5 ± 0.3 ka. At that time, the MS glacier advanced down-valley, depositing recessional moraines at 1610 m a.s.l. (Fig. 5). Although there is no evidence for similar glacier re-advances in the VS valley, synchronous moraines are preserved in other valleys in the range. Within the total uncertainties, an arithmetic mean age of 15.5 ± 1.1 ka overlaps with mean ages of 14.6 ± 1.3 ka and 14.3 ± 1.2 ka calculated based on the published ^{36}Cl exposure data (Dzierżek, 2009; Makos et al., 2014) for the

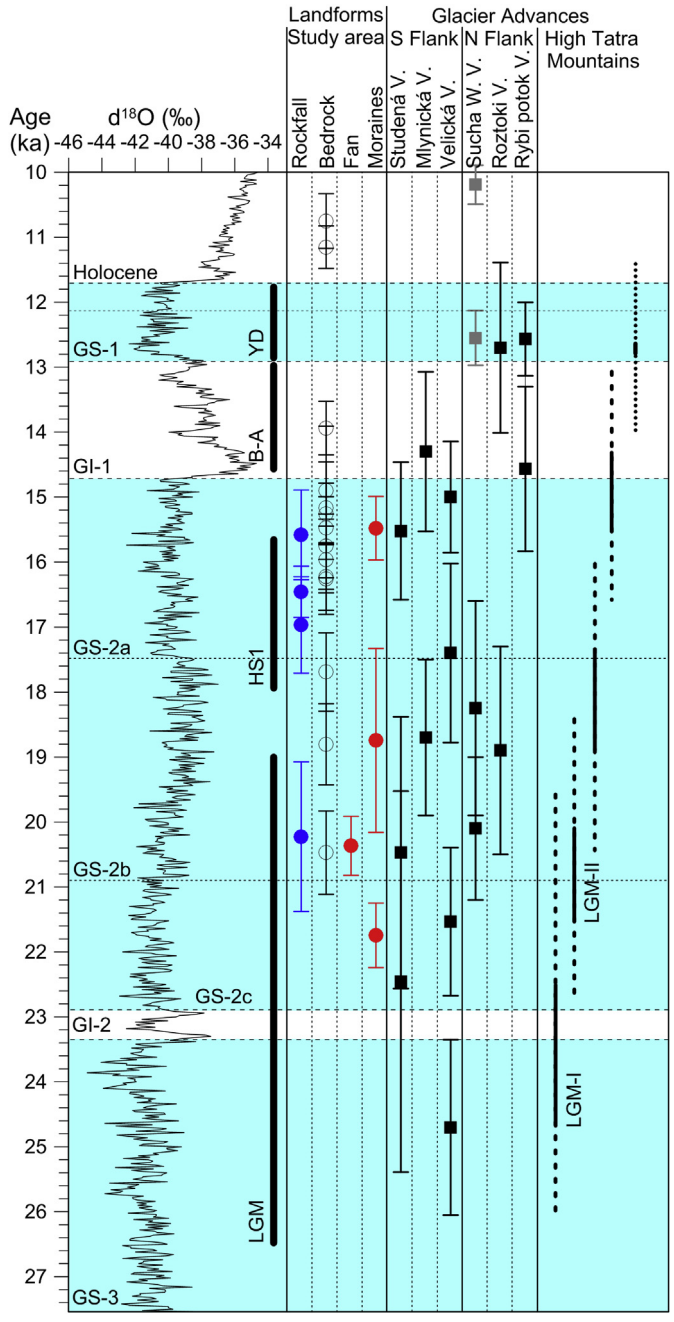

Fig. 9. ^{10}Be exposure age chronology of the last glaciation in the study area. Unfilled black circles show individual exposure ages obtained for bedrock sites and filled circles show the mean exposure ages for rockfall accumulations (blue), ice marginal fan and moraines (red). The timing of glacier advances is based on arithmetic mean exposure ages (black squares) calculated for the published ^{10}Be (this study) and ^{36}Cl (Makos et al., 2013a,b; 2014) data from the High Tatra Mts. Grey squares show ^{14}C data reported by Baumgart-Kotarba and Kotarba (2001) for moraine lakes. The time scale on the left-hand side of the figure is based on theGICC05 data for the GRIP ice core (Lowe et al., 2008; Rasmussen et al., 2014). The timing of Younger Dryas and Bølling-Allerød chronozones after Rasmussen et al. (2014), Heinrich Stadial 1 after Sanchez Goñi and Harrison (2010) and LGM after Clark et al. (2009).

Morske Oko inner moraine in the Rybi potok Valley and for the recessional moraine located at 1330 m a.s.l. in the Mlynická Valley, respectively (Fig. 9). Moreover, the exposure ages reported by Makos et al. (2014) yield a coincident mean ^{36}Cl age of 15.0 ± 0.9 ka for the recessional moraines located at 1550 m a.s.l. in the Velická Valley. Finally, the ^{14}C age of sediments from Zielony Lake in the Sucha Woda Valley indicates that the moraine dam of the lake formed well before 12.6 ± 0.4 ka (Baumgart-Kotarba and Kotarba, 2001), implying its possible origin during a regional re-advance around 15 ka. The exposure age of 15.5 ± 0.3 ka obtained from the moraine relics in the MS trough correlates well with the ^{10}Be exposure age estimate of 15.7 ± 0.6 ka and 15.3 ± 0.5 ka reported for glacier re-advances in the Bohemian Forest (Mentlík et al., 2013) and the Krkonoše Mts. (Engel et al., 2014), respectively. This re-advance phase tentatively corresponds with Gschnitz or Clavadel/Senders oscillations in the Central and Eastern Alps (e.g. Ivy-Ochs et al., 2008; Hippe et al., 2014).

The glacier re-advance around 15.5 ka was followed by deglaciation that terminated at the beginning of the Holocene. The terminus of the VS glacier retreated from the bottom of the main cirque (1974 m a.s.l.) to its upper part between 15.5 ± 0.5 and 14.9 ± 0.5 ka (Fig. 5). The youngest age from the bedrock step at 2075 m a.s.l. indicates ice-free conditions on the dam of the largest cirque lake. The position of the sample site suggests the considerably small volume of the remaining cirque glacier that probably melted soon after 14.9 ka. The early deglaciation may be attributed to the SE orientation and a widely open shape of the cirque (Fig. 2A), which precludes the effective sheltering of its surface from insolation. Relics of a small recessional moraine at 2050–2060 m a.s.l. (Fig. 4B) imply that a small glacier rejuvenated and re-advanced ~400 m down-cirque. Although the timing of this re-advance remains unknown, it could be tentatively related to local Younger Dryas (YD) ice advances that have been described within the range (Baumgart-Kotarba and Kotarba, 2001; Dzierżek, 2009; Makos et al., 2013b).

The exposure age of 13.9 ± 0.4 ka reveals the onset of the ice decay in the MS cirque that became free of glaciers around 10.7 ± 0.3 ka (Fig. 5). The age difference of ~3 ka between the MSD-02 and MSD-03 samples obtained for two elevations on the cirque step is conspicuously large considering the relatively small elevation difference of 50 m between the sample sites (Fig. 3). The substantial difference in the exposure ages may be attributed to either an unrealistically young age for the MSD-03 site or a slow retreat rate of the MS glacier. Among the factors that may lead to unrealistically young surface exposure ages, both post-glacial erosion and shielding of the sample site can be excluded. A polished and striated bedrock surface precludes significant erosion or weathering of the sample site. The shielding of the sample site by snow cover, soils or sediments seems to be improbable regarding the exposed position, southern orientation, high elevation and the relatively high dip (15°) of the sampled surface. The second hypothesis suggests that the glacier retreat rate must have been 0.05–0.08 m yr^{-1} to account for the difference in the exposure of the bedrock sites and therefore one to two orders of magnitude lower than the rates determined elsewhere in the study area. This slow rate could be explained by the terminus oscillations of the glacier at the cirque step resulting in delayed or interrupted exposure of its upper part. The hypothetical glacier re-advance or oscillations between 13.9 ± 0.4 ka and 10.7 ± 0.3 ka overlap with the YD cold period, which is recorded in the moraine sequences in the Sucha Woda, Roztoka and Za Mnichem valleys (Dzierżek, 2009; Makos et al., 2013b). Although the post-glacial shielding of the site MSD-03 cannot be completely excluded, our conclusion is that the exposure age of 10.7 ± 0.3 ka is reasonably accurate and it reflects a glacier oscillation at the cirque step during the Lateglacial/Holocene transition.

The timing of deglaciation in the study area between around 15.5 and 10.7 ka is in good agreement with the recessional periods constrained by the ^{36}Cl exposure ages at other sites within the range. The deglaciation occurred around 15–13 ka and 11–10 ka in

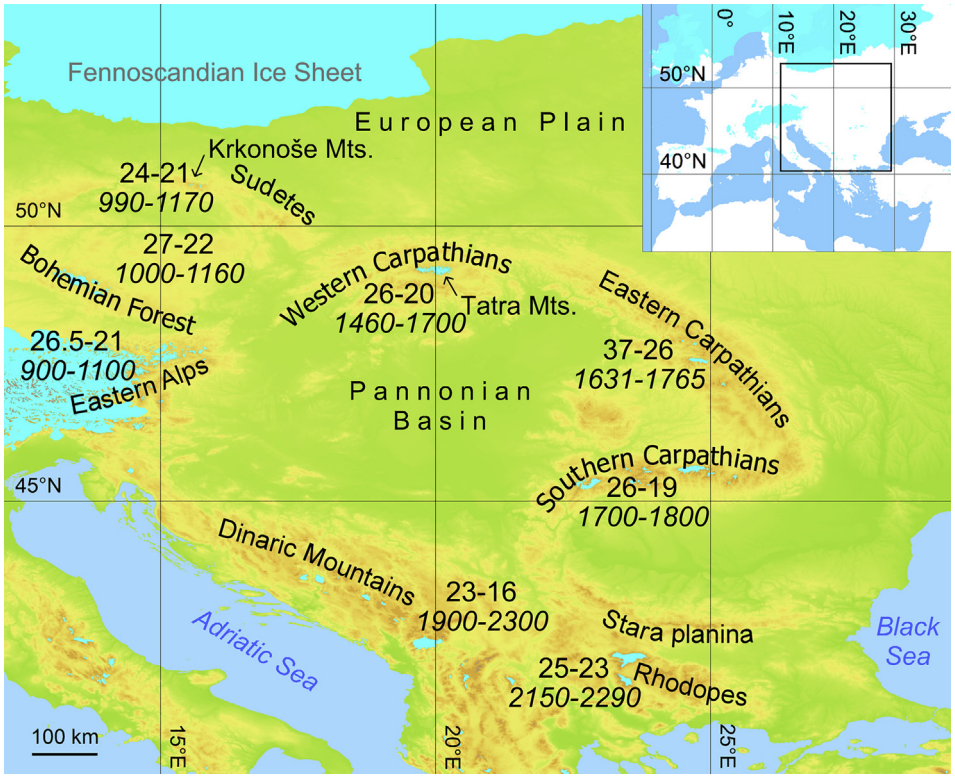

Fig. 10. Summary of published chronological data related to LGM glacier advances in Central Europe. The time (ka) and ELA (in italics) intervals after Engel (2003), Reuther (2007), Vočadlová and Křížek (2009), Kuhlemann et al. (2009, 2013a,b), László et al. (2013), Mentlík et al. (2013), Engel et al. (2014), Makos et al. (2014) and Ruszkiczay-Rüdiger et al. (2014). ETOPO1 dataset (Amante and Eakins, 2009) is used for topography. The LGM extent of ice sheet and mountain glaciers after Ehlers et al. (2011), Engel et al. (2014) and Zasadni and Kłapyta (2014).

Table 3
Morphological characteristics of former glaciers and ELAs in the study area.

^{10}Be age chronology (ka)	Lowermost point (m a.s.l.)	Surface area (km^2)	Volume		ELA (m a.s.l)	
			(km^3)	% of LGM	ssAAR$_0$	AAR 0.50
~22.0 (LGM)	970	14.04	1.21	100	(0.65) 1640	1710
>20.5	1120	12.14	0.92	76	(0.65) 1720	1790
~15.5	1680 (MS) 1920 (VS)	1.32	0.06	5	(0.55) 2130	2070
~12	2110 (MS) 2180 (VS)	0.62	0.01	0.8	(0.45) 2290	2260

the Pięciu Stawów Polskich Valley (Dzierżek, 2009), and lasted from ~15.9 to 10.9 ka in the Za Mnichem Valley (Makos et al., 2013b). The presence of small glaciers in the cirques within the VS and MS valleys (Fig. 8D) tentatively related to the YD cold period is consistent with the indices from the range. A limited extent of glaciers during the YD was initially proposed for the Sucha Woda Valley based on radiocarbon dating of the sediments from moraine-dammed lakes (Baumgart-Kotarba and Kotarba, 2001) and it has been recently confirmed by a mean ^{36}Cl exposure ages of 12.7 ± 1.3 ka and 12.6 ± 0.6 ka from moraines in the Pięciu Stawów Polskich and Za Mnichem valleys, respectively (Dzierżek, 2009; Makos et al., 2013b). The equilibrium lines in these north-facing valleys were calculated at the elevation of 1890 and 1990 m a.s.l. (Makos et al., 2013b), i.e. ~300 m lower than in the VS and MS valleys (Table 3).

The onset of deglaciation in the range is nearly synchronous with the glacier retreat following the local re-advances around 15.7 and 15.3 ka in the Bohemian Forest and the Krkonoše Mts. (Mentlík et al., 2013; Engel et al., 2014). Around the same time, glaciers started to retreat from the Clavadel/Senders moraines in the Alps (Ivy-Ochs et al., 2008). The subsequent phase of glacier recession in the Bohemian Forest and the Krkonoše Mts. (Mentlík et al., 2013; Engel et al., 2014) was interrupted by a prominent re-advance around 13.7 ka, which has not yet been chronologically constrained in either the Alps or the High Tatra Mts. The subsequent phase of ice decay in the High Tatra Mts., separated by a prominent re-advance during the YD followed by the final downwasting of the glaciers at the beginning of the Holocene, is well documented in the Krkonoše Mts., the Alps, the Eastern and the Southern Carpathians (e.g. Ivy-Ochs et al., 2009; Rinterknecht et al., 2012; Engel et al., 2014; Ruszkiczay-Rüdiger et al., 2014).

5.2. Glacier retreat and surface lowering rates

The exposure ages obtained for the bedrock surfaces offer an exceptional opportunity to determine the rate of glacier recession in the study area (Table 4). However, the average rates calculated below have to be regarded as a minimum because the period of the

Table 4
Rates of glacier retreat in the High Tatra Mountains. The retreat rates for the VS and MS valleys are based on ^{10}Be surface exposure ages for bedrock sites. ^{36}Cl exposure ages for other sites after Dzierżek et al. (1999) and Dzierżek (2009). The onset of initial glacier retreat from the Łysa Polana site was proposed by Makos et al. (2013a).

Valley	Section	Retreat rate (m yr^{-1})	Distance (m)	Sample	Elevation (m a.s.l.)	Age (yr)
Velká Studená	Trough	0.9 ± 0.5	4030	SD-04	1188	20,472 ± 1695
	Cirque step	1.9 ± 2.5	1400	VSD-09	1822	16,222 ± 521
	Cirque	0.8 ± 1.4	480	VSD-06	1974	15,476 ± 482
				VSD-05	2075	14,899 ± 463
Malá Studená	Trough	0.5 ± 0.2	3590	SD-04	1188	20,472 ± 1695
	Cirque	0.4 ± 0.1	1020	MSD-02	1994	13,939 ± 409
				MSD-01	2190	11,153 ± 435
Biała Woda/Roztoka	Trough	1.4 ± 0.3	5300	Łysa Polana	960	21,000
				T95-13WM	1090	17,300 ± 700
Pięciu Stawów Polskich	Cirque	0.2 ± 0.2	690	T95-7DPSP	1692	20,100 ± 1700
				T96-21D5SP	1637	16,600 ± 1300

overall retreat may include several oscillations or advances of the glacier termini.

The VS glacier experienced relatively rapid downwasting after the LGM. The glacier terminus started its initial retreat from the mouth of the VS trough after 20.5 ± 1.7 ka and receded ~4 km to the upper part of the trough around 16.2 ± 0.5 ka at an average retreat rate of 0.9 ± 0.5 m yr^{-1}. Subsequently, the glacier rapidly retreated above the upper edge of the trough at an average retreat rate of 1.9 ± 2.5 m yr^{-1}. This rate was double that recorded during recession in the VS trough and the highest observed in the study area. The glacier recession to the central part of the main cirque proceeded without any recognisable disruption until 15.5 ± 0.5 ka when a short glacier re-advance occurred as indicated by a small moraine at 2050–2070 m a.s.l. Thereafter, the glacier receded at an average rate of >0.8 ± 1.4 m yr^{-1} over the step of the central cirque-in-cirque form which became ice-free around 14.9 ± 0.5 ka.

In the MS hanging trough, the glacier retreated at a lower rate than in the main valley. An average rate of 0.5 ± 0.2 m yr^{-1} was determined for glacier terminus recession from the trough. However, this value has to be considered as a minimum average retreat rate because the period of overall recession after 20.5 ± 1.7 ka was interrupted by a small-scale re-advance around 15.5 ± 0.3 ka. The glacier receded from the trough until 13.9 ± 0.4 ka when the main cirque step was initially exposed. The subsequent glacier retreat in the upper MS valley decelerated as indicated by an average rate of 0.4 ± 0.1 m yr^{-1} obtained for the deglaciation of the Dolinka pod Sedielkom Valley head. The final decay of the cirque glaciers after 11.2 ± 0.4 ka was probably rapid, as no indications of a receding tongue stabilisation are found up-valley from the MSD-01 site.

The calculated average retreat rates (0.2–1.9 m yr^{-1}) fit well with the chronological data from the north-facing valleys of the range, where post-LGM deglaciation started ~21 ka (Makos et al., 2013a). Considering the distance of about 5.3 km between the LGM moraine at Łysa Polana and the dated bedrock outcrop near the Mickiewicz Waterfall (17.3 ± 0.7 ka; Dzierżek et al., 1999), the age difference of 3700 years yields an average annual retreat rate of 1.4 ± 0.3 m yr^{-1} for the Biała Woda Valley (Table 4). In the Pięciu Stawów Polskich Valley, the average retreat rate between 20.1 ± 1.7 ka and 16.6 ± 1.3 ka (Dzierżek, 2009) was 0.2 ± 0.2 m yr^{-1}. The observed rates are also in accordance with the post-LGM values reported from the Colorado Front Range (Ward et al., 2009). Finally, the rates derived in the study area are order of magnitude lower than the reported rates of the glacier retreat after YD in the Scottish Highlands (Lukas and Benn, 2006) and in the post-Little Ice Age (LIA) period in the Alps (e.g. Mazza, 1998; Zumbühl et al., 2008).

The exposure ages from the Svišťový chrbát hard rock ridge give direct evidence of the VS glacier thinning in the accumulation area between 17.7 ± 0.6 ka and 15.3 ± 0.5 ka (Fig. 6). The figures presented in Table 5 indicate that the glacier surface lowered at an average rate of centimetres per year over this period. The average thinning rate increased from 0.04 ± 0.03 m yr^{-1} to 0.09 ± 0.12 m yr^{-1} towards the end of the period. The derived range of values is in accordance with the glacier thinning rate calculated for other sites in the range based on the published exposure ages (Table 5). The ages obtained by Makos et al. (2013a) along a vertical profile in the Pusta Valley yielded a consistent rate of glacier thinning that ranged between 0.01 ± 0.01 m yr^{-1} and 0.02 ± 0.03 m yr^{-1} during Termination I. Assuming the elevation

Table 5
Glacier thinning in the High Tatra Mountains. ^{36}Cl surface exposure ages for the Pusta and Roztoka Valleys after Makos et al. (2013a) and for the Za Mnichem Valley after Makos et al. (2013b).

Valley	Transect	Sample	Elevation (m a.s.l.)	Exposure age (yr)	Thinning rate (m yr^{-1})	Period
Velká Studená	Svišťový chrbát	VSD-04	2216	17,691 ± 592	0.04 ± 0.03	GS-2a
		VSD-03	2154	16,263 ± 553	0.05 ± 0.19	
		VSD-02	2138	15,961 ± 501	0.09 ± 0.12	
		VSD-01	2077	15,258 ± 507		
Pusta	Kołowa Czuba	P-16	1991	21,500 ± 1600	0.01 ± 0.01	Post-LGM
		P-14	1973	19,100 ± 900	0.02 ± 0.03	
		P-12	1957	18,200 ± 800		
		P-11	1885	14,700 ± 700	0.01 ± 0.00	Lateglacial
		P-10	1880	11,800 ± 600		
Roztoka	Kozi Wierch	K-8	1810	16,900 ± 800	0.05 ± 0.02	GS-2a
		K-2	1637	13,500 ± 700		
Za Mnichem	Mnich	M-10	1996	15,900 ± 700	0.07 ± 0.09	GS-2a
		M-11	1937	15,000 ± 500		
	Zadni Mnich	M-5	2011	11,600 ± 600	0.15 ± 0.28	Post-YD
		M-4	1921	11,000 ± 500	0.38 ± 3.80	
		M-7	1883	10,900 ± 500		

Table 6
Average thickness changes of Alpine glaciers for the post-LIA period.

Glacier	Period	Surface lowering (m yr^{-1})	Reference
Grosser Aletschgletscher	1880–1999	0.2 to 0.8	Bauder et al., 2007
Rhonegletscher	1878–1999	0.33 to 0.87	Nishimura et al., 2013
Unteraar Glacier	1880–1997	0.24 to 0.89	Steiner et al., 2008
Unterer Grindelwald Glacier	1860–2004	0.26 to 0.90	Steiner et al., 2008
6 Alpine glaciers	1850–1985	0.1 to 0.6	Haeberli et al., 2013
20 Alpine glaciers	1900–2008	0.1 to 0.6	Huss et al., 2010

difference between the upper and lower trimlines in the Roztoka Valley and their exposure around 16.9 ka and 13.5 ka (Makos et al., 2013a), the rate of glacier thinning was 0.05 ± 0.02 m yr^{-1}. The exposure ages reported by Makos et al. (2013b) from the vertical transects in the Za Mnichem Valley yield the thinning rate of 0.07 ± 0.09 m yr^{-1} for time span 15.9–15 ka and the increased rate of 0.15 ± 0.28 m yr^{-1} for the post-YD period. The calculated values suggest that annual surface lowering in the range of centimetres was common for the accumulation zone of the valley glaciers over the post-LGM period. However, this rate is order of magnitude lower than that for the period of rapid deglaciation after the YD. Finally, the accelerated post-YD thickness changes are similar to those reported for the entire surface of Alpine glaciers since the LIA (Table 6) but generally higher than the lowering rates observed in the upper reaches of these glaciers (e.g. Bauder et al., 2007; Steiner et al., 2008; Nishimura et al., 2013).

5.3. Paraglacial accumulations

The established deglaciation chronology and the exposure ages obtained for the selected rockfall accumulations indicate that these accumulations formed within a relatively short period after the glacier retreat (Fig. 9). The rockfall accumulation located at the mouth of the VS trough coincided with the glacier retreat as indicated by a small difference between the exposure age of the adjacent SD-04 site (20.5 ± 1.7 ka) and a mean age obtained for the accumulation (20.2 ± 1.2 ka). Considering the large age uncertainties, activation of this rockfall prior to the initial ice retreat cannot be excluded. However, the undisturbed morphology of the accumulation and its position close to the valley axis suggest that this rockfall must have occurred after the retreat of the main ice body. The rockfall activity at the mouth of the MS hanging trough and in the centre of this trough occurred hundreds of years after the glacier retreat. Considering the initial deglaciation at the SD-04 site around 20.5 ka and the glacier retreat rate over the hanging trough step (0.2 ± 0.1 m yr^{-1}) and within the trough (0.5 ± 0.2 m yr^{-1}), the older and younger rockfalls occurred ~100 and 200 years after the glacier had left the trough step and the central section of the trough, respectively.

The rockfall in the upper part of the VS trough is the only sampled accumulation with a relatively long lag-time between the glacier retreat and the failure of the slopes. If the glacier wasted out of the trough at an average rate of 0.9 ± 0.5 m yr^{-1}, this failure occurred around 1400 years after the ice retreat. Although this lag-time is relatively long, it falls within the typical range of response times reported for large glacially conditioned slope failures (Prager et al., 2008; McColl, 2012; Ballantyne et al., 2014a, 2014b). Therefore, all the sampled rockfalls may be considered as resulting from (paraglacial) stress release following deglaciation (Ballantyne, 2002; Geertsema and Chiarle, 2013).

6. Conclusions

^{10}Be exposure ages from the moraines and the bedrock sites in the VS and MS valleys provide a chronology of the last glaciation on the southern flank of the High Tatra Mts. The arithmetic mean age of 22.5 ± 2.9 ka calculated for the terminal moraine in the forefield of the VS trough indicate that the maximum advance of coalesced glaciers occurred close to the global LGM. Along with the chronological data reported by Makos et al. (2014) from the Velická and Sucha Woda valleys it is possible to constrain the timing of the local LGM glacier expansion in the range to 26–20 ka. The chronology of this glacier advance is broadly synchronous with the LGM glaciation period in the Alps, the Bavarian Forest, the Krkonoše Mts. and the Southern Carpathians (Engel et al., 2011; Reuther et al., 2011; van Husen, 2011; Ruszkiczay-Rüdiger et al., 2014), but it lagged behind the period of greatest glacier extent in the Eastern Carpathians (Gheorghiu et al., 2011). The ELA of glaciers in the study area was located at 1640 m a.s.l. well within the range of ELA values reported by Makos et al. (2014) for the valleys on the southern flank of the range.

The first post-LGM glacier re-advance occurred no later than 20.5 ± 1.7 ka when the glacier terminated at the mouth of the VS trough. The timing and largest extent of the initial post-LGM re-advance is in accordance with glacier expansion in the Sucha Woda, Velická and Mlynická valleys where the glaciers advanced prior to ~19 ka terminating close to the LGM moraines (Makos et al., 2014). This re-advance is also consistent with the younger LGM glacier expansion in the Alps, the Bavarian/Bohemian Forest and the Krkonoše Mts. (Starnberger et al., 2011; Mentlík et al., 2013; Engel et al., 2014). The onset of the glacier recession in the study area around 20.5 ka constrains the timing of post-LGM deglaciation in the High Tatra Mts., which lasted until 18–17 ka (Makos et al., 2013a). The subsequent period of an overall glacier recession was interrupted by glacier re-advance in the central section of the troughs no later than 15.5 ± 1.1 ka. This re-advance is broadly synchronous with the glacier expansion in the Velická, Mlynická, Rybi potok and Sucha Woda valleys (Baumgart-Kotarba and Kotarba, 2001; Dzierżek, 2009; Makos et al., 2014) and it also correlates with glacier advances in the Central and Eastern Alps, the Bohemian Forest and the Krkonoše Mts. during the Lateglacial (Mentlík et al., 2013; Engel et al., 2014; Hippe et al., 2014).

During the YD cold period, glaciers were restricted to the upper parts of the investigated valleys. In the MS Valley, glacier termini descended slightly out of the cirque-in-cirque forms and retreated back over the cirque steps around 11.2–10.7 ka. The limited extent of the YD glaciers in the range was initially proposed for the Sucha Woda Valley based on radiocarbon dating of the moraine-dammed lakes (Baumgart-Kotarba and Kotarba, 2001). This concept has been recently confirmed by a mean ^{36}Cl exposure ages of ~12.5 ka reported from the moraines in the Roztoka and Za Mnichem valleys (Dzierżek, 2009; Makos et al., 2013b). The retreat of glaciers after ~11 ka in the range is in accordance with the onset of the post-YD glacier recession in central European mountains including the Alps, the Krkonoše Mts. and the Carpathians (e.g. Ivy-Ochs et al., 2009; Engel et al., 2014; Ruszkiczay-Rüdiger et al., 2014).

The cosmogenic data allowed for the reconstruction of glacier retreat and thinning in the study area. These data demonstrate that

during the progressive ice decay between 20.5 ± 1.7 and 16.2 ± 0.5 ka the VS glacier receded ~4 km up-valley at the average retreat rate of 0.9 ± 0.5 m yr^{-1}. The subsequent retreat from the trough occurred at a significantly higher rate of 1.9 ± 2.5 m yr^{-1} whereas the final recession in cirque probably decelerated to 0.8 ± 1.4 m yr^{-1}. The same order of magnitude was determined for the retreat of the MS glacier in both the trough and the cirque areas. The observed retreat rates are in accordance with the values calculated for the post-LGM recession in the Pięciu Stawów Polskich and Biała Woda/Roztoka valleys in the northern part of the range based on the previously published ^{36}Cl exposure ages (Dzierżek et al., 1999; Dzierżek, 2009).

The exposure ages from the VS valley indicate that the glacier surface lowered at an average rate of centimetres per year between 17.7 ka and 15.3 ka. The average thinning rate increased from 0.04 ± 0.03 m yr^{-1} to 0.09 ± 0.12 m yr^{-1} towards the end of the period. These values are well within the range of the post-LGM glacier thinning rate calculated for the High Tatra Mts. based on the ^{36}Cl exposure ages published by Makos et al. (2013a,b). The combination of our data and recently published exposure ages from the Za Mnichem Valley (Makos et al., 2013b) allows us to suggest that post-LGM glacier downwasting in the range was an order of magnitude lower than during the post-YD period. During the latter period, glacier surfaces lowered by tenths of a metre per year, which is a rate that has been observed since the termination of the LIA in the Alps.

The established chronology of the glacier retreat and the exposure data obtained for rockfall accumulations in the VS and MS valleys suggest that the major rockfall events in the study area are glacially conditioned. The timing of the sampled rockfalls around 20.2 ka, and between 17.0 and 16.5 ka is synchronous with the deglaciation periods and hundreds of years after glacier retreat. The rockfall failure around 15.6 ka occurred more than a thousand years after the glacier had left, but probably also as a result of glacial debuttressing. The combination of the exposure data from both glacial landforms and rockfall accumulations represents the first chronological evidence of paraglacial processes in the High Tatra Mts. These data also represent one of few direct constraints of rockfall accumulations conditioned by the post-LGM retreat of mountain glaciers.

Acknowledgements

This study is part of the ESF EUROCORES TOPO-EUROPE CRP “Source to Sink” project supported by the Slovak Research and Development Agency under the contracts APVV ESFEC-0006-07 and APVV-0625-11. The fieldwork and laboratory analyses were supported by the Czech Science Foundation (projects P209/10/0519 and 13-15123S). The largest ASTER AMS national facility (CEREGE, Aix en Provence) is supported by the INSU/CNRS, the French Ministry of Research and Higher Education, IRD and CEA. The authors acknowledge the Tatra National Park Authorities for providing permission to work in the region. We are grateful for text corrections from Simon M. Hutchinson (University of Salford) and for constructive referee comments from Martin Margold (Durham University) and Daniel Nývlt (Masaryk University).

References

Amante, C., Eakins, B.W., 2009. ETOPO1 1 Arc-minute Global Relief Model: Procedures, Data Sources and Analysis. NOAA, Boulder.
Arnold, M., Merchel, S., Bourlès, D.L., Braucher, R., Benedetti, L., Finkel, R.C., Aumaître, G., Gottdang, A., Klein, M., 2010. The French accelerator mass spectrometry facility ASTER: improved performance and developments. Nucl. Instrum. Methods Phys. Res. Sect. B 268, 1954–1959.
Balco, G., 2011. Contributions and unrealized potential contributions of cosmogenic nuclide exposure dating to glacier chronology, 1990–2010. Quat. Sci. Rev. 30, 3–27.
Balco, G., Briner, J., Finkel, R.C., Rayburn, J.A., Ridge, J.C., Schaefer, J.M., 2009. Regional beryllium-10 production rate calibration for late-glacial northeastern North America. Quat. Geochronol. 4 (2), 93–107.
Ballantyne, C.K., 2002. Paraglacial geomorphology. Quat. Sci. Rev. 21 (18–19), 1935–2017.
Ballantyne, C.K., Sandeman, G.F., Stone, J.O., Wilson, P., 2014a. Rock-slope failure following Late Pleistocene deglaciation on tectonically stable mountainous terrain. Quat. Sci. Rev. 86, 144–157.
Ballantyne, C.K., Wilson, P., Gheorghiu, D., Rodés, A., 2014b. Enhanced rock-slope failure following ice-sheet deglaciation: timing and causes. Earth Surf. Process. Landf. 39, 900–913.
Bauder, A., Funk, M., Huss, M., 2007. Ice-volume changes of selected glaciers in the Swiss Alps since the end of the 19th century. Ann. Glaciol. 46, 145–149.
Baumgart-Kotarba, M., Kotarba, A., 1993. Późnoglacjalne i holoceńskie osady z Czarnego Stawu Gąsienicowego w Tatrach. Dok. Geogr. 4–5, 9–30.
Baumgart-Kotarba, M., Kotarba, A., 1995. High Mountain environment of the Tatras in the period of Pleistocene and Holocene transition. B. Peryglac. 34, 37–51.
Baumgart-Kotarba, M., Kotarba, A., 1997. Würm glaciation in the Biała Woda Valley, High Tatra Mountains. Stud. Geomorph. Carpatho-Balcan 31, 57–81.
Baumgart-Kotarba, M., Kotarba, A., 2001. Deglaciation of the Sucha Woda and Pańszczyca valleys in the Polish High Tatras. Stud. Geomorph. Carpatho-Balcan. 35, 7–38.
Benn, D.I., Owen, L.A., Osmaston, H.A., Seltzer, G.O., Porter, S.C., Mark, B., 2005. Reconstruction of equilibrium-line altitudes for tropical and sub-tropical glaciers. Quatern. Int. 138–139, 8–21.
Braucher, R., Bourlès, D., Merchel, S., Vidal Romani, J., Fernadez-Mosquera, D., Marti, K., Léanni, L., Chauvet, F., Arnold, M., Aumaître, G., Keddadouche, K., 2013. Determination of muon attenuation lengths in depth profiles from in situ produced cosmogenic nuclides. Nucl. Instrum. Methods Phys. Res. Sect. B Beam Interact. Mater. Atoms 294, 484–490.
Briner, J.P., 2009. Moraine pebbles and boulders yield indistinguishable ^{10}Be ages: a case study from Colorado, USA. Quat. Geochronol. 4 (4), 299–305.
Briner, J.P., Swanson, T.W., Caffee, M., 2001. Late Pleistocene cosmogenic ^{36}Cl glacial chronology of the southwestern Ahklun Mountains, Alaska. Quat. Res. 56 (2), 148–154.
Briner, J.P., Kaufman, D.S., Manley, W.F., Finkel, R.C., Caffee, M.W., 2005. Cosmogenic exposure dating of late Pleistocene moraine stabilization in Alaska. Geol. Soc. Am. Bull. 117 (7–8), 1108–1120.
Briner, J.P., Bini, A.C., Anderson, R.S., 2009. Rapid early Holocene retreat of a Laurentide outlet glacier through an Arctic fjord. Nat. Geosci. 2 (7), 496–499.
Briner, J.P., Young, N.E., Goehring, B.M., Schaefer, J.M., 2012. Constraining Holocene ^{10}Be production rates in Greenland. J. Quat. Sci. 27 (1), 2–6.
Butrym, J., Lindner, L., Okszos, D., 1990. Formy rzeźby, wiek TL osadów i rozwój lodowców ostatniego zlodowacenia w Dolinie Małej Łąki, Tatry Zachodnie. Prz. Geol. 38 (1), 20–26.
Carr, S., Coleman, C., 2007. An improved technique for the reconstruction of former glacier mass-balance and dynamics. Geomorphology 92 (1–2), 76–90.
Chmeleff, J., von Blanckenburg, F., Kossert, K., Jakob, D., 2010. Determination of the ^{10}Be half-life by multicollector ICP-MS and liquid scintillation counting. Nucl. Instr. Meth. B 263 (2), 192–199.
Clark, P.U., Dyke, A.S., Shakun, J.D., Carlson, A.E., Clark, J., Wohlfarth, B., Mitrovica, J.X., Hostetler, S.W., McCabe, A.M., 2009. The Last Glacial Maximum. Science 325 (5941), 710–713.
de Martonne, E., 1911. Etude morphologique des Alpes orientales (Tauern) et des Karpates septentrionales (Tatra). Bull. Géog. Hist. 3, 387–406.
Delunel, R., Hantz, D., Braucher, R., Bourlès, D.L., Schoeneich, I.P., Depariset, I.J., 2010. Surface exposure dating and geophysical prospecting of the Holocene Lauvitel rock slide (French Alps). Landslides 7 (4), 393–400.
Dénes, F., 1902. Die Geologie des Tatragebirges. Jahrb. Ung. Karpathen-Vereins 29, 53–114.
Dielforder, A., Hetzel, R., 2014. The deglaciation history of the Simplon region (southern Swiss Alps) constrained by ^{10}Be exposure dating of ice-molded bedrock surfaces. Quat. Sci. Rev. 84, 26–38.
Dunai, T.J., 2010. Cosmogenic Nuclides – Principles, Concepts and Applications in the Earth Surface Sciences. Cambridge University Press, New York.
Dunne, J., Elmore, D., Muzikar, P., 1999. Scaling factors for the rates of production of cosmogenic nuclides for geometric shielding and attenuation at depth on sloped surfaces. Geomorphology 27 (1–2), 3–11.
Dyke, L.M., Hughes, A.L.C., Murray, T., Hiemstra, J.F., Andresen, C.S., Rodés, A., 2014. Evidence for the asynchronous retreat of large outlet glaciers in southeast Greenland at the end of the last glaciation. Quat. Sci. Rev. 99, 244–259.
Dzierżek, J., 2009. Paleogeografia wybranych obszarów Polski w czasie ostatniego zlodowacenia. Acta Geogr. Lodz. 95, 1–112.
Dzierżek, J., Nitychoruk, J., Zreda, M.G., Zreda-Gostyńska, G., 1999. Metoda datowania kosmogenicznym izotopem ^{36}Cl – nowe dane do chronologii glacjalnej Tatr Wysokich. Prz. Geol. 47 (11), 987–992.
Ehlers, J., Gibbard, P.L., Hughes, P.D. (Eds.), 2011. Quaternary Glaciations – Extent and Chronology: a Closer Look. Developments in Quaternary Science. Elsevier, Amsterdam.
Engel, Z., 2003. Pleistocénní zalednění české části Krkonoš. Przyr. Sudet. Zach. 6, 223–234.
Engel, Z., Traczyk, A., Braucher, R., Woronko, B., Křížek, M., 2011. Use of ^{10}Be exposure ages and Schmidt hammer data for correlation of moraines in the

Krkonoše Mountains, Poland/Czech Republic. Z. Geomorphol. 55 (2), 175–196.
Engel, Z., Braucher, R., Traczyk, A., Laetitia, L., ASTER team, 2014. ^{10}Be exposure age chronology of the last glaciation in the Krkonoše Mountains, Central Europe. Geomorphology 206, 107–121.
Favilli, F., Egli, M., Brandová, D., Ivy-Ochs, S., Kubik, P.W., Cherubini, P., Mirabella, A., Sartori, G., Giaccai, D., Haeberli, W., 2009. Combined use of relative and absolute dating techniques for detecting signals of Alpine landscape evolution during the late Pleistocene and early Holocene. Geomorphology 112 (1–2), 48–66.
Fenton, C.R., Hermanns, R.L., Blikra, L.H., Kubik, P.W., Bryant, C., Niedermann, S., Meixner, A., Goethals, M.M., 2011. Regional ^{10}Be production rate calibration for the past 12 ka deduced from the radiocarbon-dated Grøtlandsura and Russenes rock avalanches at 69°N. Nor. Quat. Geochronol. 6 (5), 437–452.
Gądek, B., 2008. The problem of firn-ice patches in the Polish Tatras as an indicator of climatic fluctuations. Geogr. Pol. 81 (1), 41–52.
Geertsema, M., Chiarle, M., 2013. Mass movement: effects of glacial thinning. In: Shroder, J.F. (Ed.), Treatise on Geomorphology. Academic Press, San Diego, pp. 217–222.
Gheorghiu, D., Fabel, D., Xu, S., 2011. Cosmogenic ^{10}Be Constraints on the Deglaciation History in the Rodna Mountains, Northern Romania. Climate Change in the Carpathian-Balkan Region during the Late Pleistocene and Holocene. Book of Abstracts, Suceava, p. 33.
Goehring, B.M., Lohne, Ø.S., Mangerud, J., Svendsen, J.I., Gyllencreutz, R., Schaefer, J., Finkel, R., 2012. Late Glacial and Holocene beryllium-10 production rates for western Norway. J. Quat. Sci. 27 (1), 89–96.
Gosse, J.C., 2005. The contributions of cosmogenic nuclides to unraveling alpine paleo-glacier histories. In: Huber, U.M., Bugmann, H.K.M., Reasoner, M.A. (Eds.), Global Change and Mountain Regions: an Overview of Current Knowledge. Springer, Dordrecht, pp. 39–50.
Gosse, J.C., Phillips, F.M., 2001. Terrestrial in situ cosmogenic nuclides: theory and application. Quat. Sci. Rev. 20 (14), 1475–1560.
Gosse, J.C., Evenson, E.B., Klein, J., Lawn, B., Middleton, R., 1995. Precise cosmogenic ^{10}Be measurements in western North America: support fort a global Younger Dryas cooling event. Geology 23 (10), 877–880.
Haeberli, W., Paul, F., Zemp, M., 2013. Vanishing glaciers in the European Alps. In: Crutzen, P.J., Bengtsson, L., Ramanathan, V. (Eds.), Fate of Mountain Glaciers in the Anthropocene, Scripta Varia, vol. 118. The Pontifical Academy of Sciences, Vatican, pp. 1–9.
Halicki, B., 1930. Dyluwialne zlodowacenie północnych stoków Tatr. Spraw. Pol. Inst. Geol. 5 (3–4), 375–534.
Hallet, B., Putkonen, J.K., 1994. Surface dating of dynamic landforms: young boulders on aging moraines. Science 265 (5174), 937–940.
Hess, M., 1996. Klimat. In: Mirek, Z. (Ed.), Przyroda Tatrzańskiego Parku Narodowego. TPN, Kraków-Zakopane, pp. 53–69.
Heyman, J., Stroeven, A.P., Harbor, J.M., Caffee, M.W., 2011. Too young or too old: evaluating cosmogenic exposure dating based on an analysis of compiled boulder exposure ages. Earth Planet. Sci. Lett. 302, 71–80.
Heyman, B.M., Heyman, J., Fickert, T., Harbor, J.M., 2013. Paleo-climate of the central European uplands during the last glacial maximum based on glacier mass-balance modelling. Quat. Res. 79 (1), 49–54.
Hippe, K., Ivy-Ochs, S., Kober, F., Zasadni, J., Wieler, R., Wacker, L., Kubik, P.W., Schlüchter, C., 2014. Chronology of Lateglacial ice flow reorganization and deglaciation in the Gotthard Pass area, Central Swiss Alps, based on cosmogenic ^{10}Be and in situ ^{14}C. Quat. Geochronol. 19, 14–26.
Hughes, P.D., 2010. Little Ice Age glaciers in the Balkans: low altitude glaciation enabled by cooler temperatures and local topoclimatic controls. Earth Surf. Process. Landf. 35 (2), 229–241.
Hughes, P.D., Gibbard, P.L., Ehlers, J., 2013. Timing of glaciation during the last glacial cycle: evaluating the meaning and significance of the 'Last Glacial Maximum' (LGM). Earth Sci. Rev. 125, 171–198.
Huss, M., Usselmann, S., Farinotti, D., Bauder, A., 2010. Glacier mass balance in the south-eastern Swiss Alps since 1900 and perspectives for the future. Erdkunde 65 (2), 119–140.
Ivy-Ochs, S., Kober, F., 2008. Surface exposure dating with cosmogenic nuclides. Eiszeitalt. Ggw 57 (1–2), 179–209.
Ivy-Ochs, S., Schäfer, J., Kubik, P.W., Synal, H.A., Schlüchter, C., 2004. Timing of deglaciation on the northern Alpine foreland (Switzerland). Eclogae Geol. Helv. 97 (1), 47–55.
Ivy-Ochs, S., Kerschner, H., Schlüchter, C., 2007. Cosmogenic nuclides and the dating of Lateglacial and Early Holocene glacier variations: the Alpine perspective. Quatern. Int. 164–165, 53–63.
Ivy-Ochs, S., Kerschner, H., Reuther, A., Preusser, F., Heine, K., Maisch, M., Kubik, P.W., Schlüchter, C., 2008. Chronology of the last glacial cycle in the European Alps. J. Quat. Sci. 23 (6–7), 559–573.
Ivy-Ochs, S., Kerschner, H., Maisch, M., Christl, M., Kubik, P.W., Schlüchter, C., 2009. Latest Pleistocene and Holocene glacier variations in the European Alps. Quat. Sci. Rev. 28 (21–22), 2137–2149.
Jurewicz, E., 2007. Multistage evolution of the granitoid core in Tatra Mountains. In: Kozłowski, A., Wiszniewska, J. (Eds.), Granitoids in Poland. Warsaw University, Warsaw, pp. 307–317.
Kelly, M., Ivy-Ochs, S., Kubik, P., von Blanckenburg, F., Schlüchter, C., 2006. Chronology of deglaciation based on ^{10}Be dates of glacial erosional features in the Grimsel Pass region, central Swiss Alps. Boreas 35 (4), 634–643.
Kern, Z., László, P., 2010. Size specific steady-state accumulation area ratio: an improvement for equilibrium line estimation of small paleoglaciers. Quat. Sci. Rev. 29 (19–20), 2781–2787.
Kerschner, H., Ivy-Ochs, S., 2008. Palaeoclimate from glaciers: examples from the Eastern Alps during the Alpine Lateglacial and early Holocene. Glob. Planet. Change 60 (1–2), 58–71.
Klimaszewski, M., 1960. On the influence of pre-glacial relief on the extension and development of glaciation and deglaciation of mountainous regions. Prz. Geogr. 32, 41–49.
Kočický, D., 1996. Charakteristiky snehovej pokrývky v oblasti Tatier v období 1960/61–1989/90. Unpublished diploma thesis. Comenius University in Bratislava.
Korschinek, G., Bergmaier, A., Faestermann, T., Gerstmann, U.C., Knie, K., Rugel, G., Wallner, A., 2010. A new value for the half-life of ^{10}Be by heavy-ion elastic recoil detection and liquid scintillation counting. Nucl. Instr. Meth. B 268 (2), 187–191.
Králiková, S., Vojtko, R., Andriessen, R., Kováč, M., Fügenschuh, B., Hók, J., Minár, J., 2014. Cretaceous-Quaternary tectonic evolution of the Tatra Mts (Western Carpathians): constraints from structural, sedimentary, geomorphological, and fission track data. Geol. Carpath. 65 (4), 307–326.
Krupiński, K.M., 1984. Evolution of Late Glacial and Holocene vegetation in the Polish Tatra Mts., based on pollen analysis of sediments of the Przedni Staw Lake. B. Pol. Acad. Sci.-Earth 31, 37–48.
Kuhlemann, J., Milivojević, M., Krumrei, I., Kubik, P., 2009. Last glaciation of the Šara Range (Balkan Peninsula): Increasing dryness from the LGM to the Holocene. Austrian J. Earth Sci. 102, 146–158.
Kuhlemann, J., Dobre, F., Urdea, P., Krumrei, I., Gachev, E., Kubik, P., Rahn, M., 2013a. Last Glacial Maximum glaciation of the Central South Carpathian Range (Romania). Austrian J. Earth Sci. 106, 83–95.
Kuhlemann, J., Gachev, E., Gikov, A., Nedkov, S., Krumrei, I., Kubik, P., 2013b. Glaciation in the Rila Mountains (Bulgaria) during the Last Glacial Maximum. Quatern. Int. 293, 51–62.
László, P., Kern, Z., Nagy, B., 2013. Late Pleistocene glaciers in the western Rodna Mountains, Romania. Quat. Int. 293, 79–91.
Lindner, L., 1994. Jednostki stadialne i interstadialne ostatniego zlodowacenia (Würm, Vistulian) w Tatrach Polskich i na Podhalu. Acta Univ. Nicolai Copernici Geogr. 27 (92), 59–73.
Lindner, L., Dzierżek, J., Nitychoruk, J., 1990. Problem wieku i zasięgu lodowców ostatniego zlodowacenia (Vistulian) w Tatrach Polskich. Geol. Quart. 34 (2), 339–354.
Lindner, L., Nitychoruk, J., Butrym, J., 1993. Liczba i wiek zlodowaceń tatrzańskich w świetle datowań termoluminescencyjnych osadów wodnolodowcowych w dorzeczu Białego Dunajca. Prz. Geol. 41 (1), 10–21.
Lowe, J.J., Rasmussen, S.O., Bjorck, S., Hoek, W.Z., Steffensen, J.P., Walker, M.J.C., Yu, Z.C., Grp, I., 2008. Synchronisation of palaeoenvironmental events in the North Atlantic region during the Last Termination: a revised protocol recommended by the INTIMATE group. Quat. Sci. Rev. 27, 6–17.
Luckman, B.H., 2013. Processes, transport, deposition, and landforms: rockfall. In: Shroder, J.F. (Ed.), Treatise on Geomorphology. Elsevier, Oxford, pp. 174–182.
Lukas, S., Benn, D.I., 2006. Retreat dynamics of Younger Dryas glaciers in the far NW Scottish Highlands reconstructed from moraine sequences. Scot. Geogr. J. 122, 308–325.
Lukniš, M., 1959. Reliéf a roztriedenie kvartérnych útvarov vo Vysokých Tatrách a na ich predpolí. Geol. sborník 10 (1), 233–258.
Lukniš, M., 1964. The course of the last glaciation of the Western Carpathians in the relation to the Alps, to the glaciation of northern Europe, and to the division of the central European Würm into periods. Geogr. časopis 16 (2), 127–142.
Lukniš, M., 1973. Reliéf Vysokých Tatier a ich predpolia. Veda, Bratislava.
Makos, M., Nitychoruk, J., Zreda, M., 2013a. Deglaciation chronology and paleo-climate of the Pięciu Stawów Polskich/Roztoki Valley, High Tatra Mountains, Western Carpathians since the Last Glacial Maximum, inferred from ^{36}Cl exposure dating and glacier–climate modelling. Quatern. Int. 293, 63–78.
Makos, M., Nitychoruk, J., Zreda, M., 2013b. The Younger Dryas climatic conditions in the Za Mnichem Valley (Polish High Tatra Mountains) based on exposure-age dating and glacier–climate modelling. Boreas 42 (3), 745–761.
Makos, M., Dzierżek, J., Nitychoruk, J., Zreda, M., 2014. Timing of glacier advances and climate in the High Tatra Mountains (Western Carpathians) during the Last Glacial Maximum. Quat. Res. 82 (1), 1–13.
Masarik, J., Weiler, R., 2003. Production rates of cosmogenic nuclides in boulders. Earth Planet. Sci. Lett. 216 (1–2), 201–208.
Mazza, A., 1998. Evolution and dynamics of Ghiacciaio Nord delle Locce (Valle Anzasca, Western Alps) from 1854 to the present. Geogr. Fis. Din. Quat. 21 (2), 233–243.
McColl, S., 2012. Paraglacial rock-slope stability. Geomorphology 153–154, 1–16.
Mentlík, P., Engel, Z., Braucher, R., Léanni, K., Aster Team, 2013. Chronology of the Late Weichselian glaciation in the Bohemian Forest in Central Europe. Quat. Sci. Rev. 65, 120–128.
Moon, B.P., 1984. Refinement of a technique for determining rock mass strength for geomorphological purposes. Earth Surf. Process. Landf. 9 (2), 189–193.
Nemčok, J., Bezák, V., Biely, A., Gorek, A., Gross, P., Halouzka, R., Janák, M., Kahan, Š., Mello, J., Reichwalder, P., Zelman, J., 1994. Geological Map of the High Tatra Mountains 1:50 000 Scale. Geologický ústav Dionýza Štúra, Bratislava.
Niedźwiedź, T., 1992. Climate of the Tatra Mountains. Mt. Res. Dev. 12, 131–146.
Nishimura, D., Sugiyama, S., Bauder, A., Funk, M., 2013. Changes in ice-flow velocity and surface elevation from 1874 to 2006 in Rhonegletscher, Switzerland. Arct. Antarct. Alp. Res. 45 (4), 552–562.
Partsch, J., 1882. Die Gletscher der Vorzeit in den Karpathen und den Mittlegebirgen Deutschlands. Wilhelm Koebner, Breslau.
Partsch, J., 1907. Die Hohe Tatra zur Eiszeit. Berichte der philol. history. Kl. Kgl. Sächs. Ges. Wiss. 60, 177–194.

Partsch, J., 1923. Die Hohe Tatra zur Eiszeit. Ferdinand Hirt & Sohn, Leipzig.
Pellegrini, G.B., Albanese, D., Bertoldi, R., Surian, N., 2005. La deglaciazione alpina nel Vallone Bellunese, Alpi meridionali orientali. Geogr. Fis. Din. Quat. Suppl. 7, 271–280.
Phillips, F.M., Zreda, M.G., Smith, S.S., Elmore, D., Kubik, P.W., Sharma, P., 1990. Cosmogenic chlorine-36 chronology for glacial deposits at Bloody Canyon, Eastern Sierra Nevada. Science 248 (4962), 1529–1532.
Prager, C., Zangerl, C., Patzelt, G., Brandner, R., 2008. Age distribution of fossil landslides in the Tyrol (Austria) and its surrounding areas. Nat. Hazards Earth Syst. Sci. 8, 377–407.
Preusser, F., 2004. Towards a chronology of the Late Pleistocene in the northern Alpine Foreland. Boreas 33, 195–210.
Preusser, F., Graf, H.R., Keller, O., Krayss, E., Schlüchter, C., 2011. Quaternary Glaciation history of northern Switzerland. Eiszeitalt. Ggw. 60, 282–305.
Prószyńska-Bordas, H., Stańska-Prószyńska, W., Prószyński, M., 1988. TL dating of partially bleached sediments by the regeneration method. Quat. Sci. Rev. 7, 265–271.
Putiš, M., 1992. Variscan and Alpidic nappe structures of the Western Carpathian crystalline basement. Geol. Carpath. 43 (6), 369–380.
Putkonen, J., Swanson, T., 2003. Accuracy of cosmogenic ages for moraines. Quat. Res. 59 (2), 255–261.
Rasmussen, S.O., Bigler, M., Blockley, S., Blunier, T., Buchardt, B., Clausen, H., Cvijanovic, I., Dahl-Jensen, D., Johnsen, S., Fischer, H., Gkinis, V., Guillevic, M., Hoek, W., Lowe, J., Pedro, J., Popp, T., Seierstad, I., Steffensen, J., Svensson, A., Vallelonga, P., Vinther, B., Walker, M., Wheatley, J.J., Winstrup, M., 2014. A stratigraphic framework for abrupt climatic changes during the Last Glacial period based on three synchronized Greenland ice-core records: refining and extending the INTIMATE event stratigraphy. Quat. Sci. Rev. 106, 14–28.
Reitner, J.M., 2007. Glacial dynamics at the beginning of Termination I in the Eastern Alps and their stratigraphic implications. Quatern. Int. 164–165, 64–84.
Reuther, A.U., 2007. Surface Exposure Dating of Glacial Deposits from the Last Glacial Cycle: Evidence from the Eastern Alps, the Bavarian Forest, the Southern Carpathians and the Altai Mountains. Gebr. Borntraeger, Berlin.
Reuther, A.U., Fiebig, M., Ivy-Ochs, S., Kubik, P.W., Reitner, J.M., Jerz, H., Heine, K., 2011. Deglaciation of a large piedmont lobe glacier in comparison with a small mountain glacier – new insight from surface exposure dating. Two studies from SE Germany. Quat. Sci. J. 60 (2–3), 248–269.
Rinterknecht, V.R., Clark, P.U., Raisbeck, G.M., Yiou, F., Bitinas, A., Brook, E.J., Marks, L., Zelcs, V., Lunka, J.P., Pavlovskaya, I.E., Piotrowski, J.A., Raukas, A., 2006. The last deglaciation of the Southeastern sector of the Scandinavian Ice Sheet. Science 311 (5766), 1449–1452.
Rinterknecht, V., Matoshko, A., Gorokhovich, Y., Fabel, D., Xu, S., 2012. Expression of the Younger Dryas cold event in the Carpathian Mountains, Ukraine? Quat. Sci. Rev. 39, 106–114.
Romer, E., 1929. Tatrzańska Epoka Lodowa. Księgarnie Sp. Akc. Książnica-Atlas, Lwów.
Ruszkiczay-Rüdiger, Z., Kern, Z., Urdea, P., Braucher, R., Schimmelpfennig, I., 2014. (Un)Resolved contradictions in the Late Pleistocene glacial chronology of the Southern Carpathians – new samples and recalculated cosmogenic radionuclide age estimates. In: Mindrescu, M. (Ed.), Late Pleistocene and Holocene Climatic Variability in the Carpathian-Balkan Region 2014. Stefan cel Mare University Press, Suceava, pp. 152–156.
Sanchez Goñi, M.F., Harrison, S.P., 2010. Millennial-scale climate variability and vegetation changes during the Last Glacial: concepts and terminology. Quat. Sci. Rev. 29, 2823–2827.
Starnberger, R., Rodnight, H., Spötl, C., 2011. Chronology of the Last Glacial Maximum in the Salzach Palaeoglacier Area (Eastern Alps). J. Quat. Sci. 26 (5), 502–510.
Steiner, D., Zumbühl, H.J., Bauder, A., 2008. Two Alpine glaciers over the past two centuries: a scientific view based on pictorial sources. In: Orlove, B., Wiegandt, E., Luckman, B.H. (Eds.), Darkening Peaks: Glacier Retreat, Science, and Society. University of California Press, Berkeley, pp. 83–99.
Stone, J.O., 2000. Air pressure and cosmogenic isotope production. J. Geophys. Res. 105 (B10), 23753–23759.
Stone, J.O., Balco, G.A., Sugden, D.E., Caffee, M.W., Sass, L.C., Cowderry, S.G., Siddoway, C., 2003. Holocene deglaciation of Marie Bird Land, West Antarctica. Science 299 (5603), 99–102.
Tschudi, S., Ivy-Ochs, S., Schlüchter, C., Kubik, P., Rainio, H., 2000. ^{10}Be dating of Younger Dryas Salpausselkä I formation in Finland. Boreas 29 (4), 287–293.
UNEP, 2007. Carpathians Environment Outlook. UNEP, Geneva.
van Husen, D., 2011. Quaternary glaciations in Austria. In: Ehlers, J., Gibbard, P.L., Hughes, P.D. (Eds.), Quaternary Glaciations – Extent and Chronology. Elsevier, Amsterdam, pp. 15–28.
Vermeesch, P., 2012. On the visualisation of detrital age distributions. Chem. Geol. 312–313, 190–194.
Vočadlová, K., Křížek, M., 2009. Comparison of glacial relief landforms and the factors which determine glaciation in the surroundings of Černé jezero Lake and Čertovo jezero Lake (Šumava Mts., Czech Republic). Morav. Geogr. Rep. 17 (2), 2–14.
Ward, G.K., Wilson, S.R., 1978. Procedures for comparing and combining radiocarbon age determinations: a critique. Archaeometry 20 (1), 19–31.
Ward, D.J., Anderson, R.S., Guido, Z.S., Briner, J.P., 2009. Numerical modeling of cosmogenic deglaciation records, Front Range and San Juan Mountains, Colorado. J. Geophys. Res. 114, F01026.
Zasadni, J., Kłapyta, P., 2009. An attempt to assess the modern and Little Ice Age climatic snowline altitude in the Tatra Mountains. Landf. Anal. 10, 124–133.
Zasadni, J., Kłapyta, P., 2014. The Tatra Mountains during the Last Glacial Maximum. J. Maps 10 (3), 440–456.
Zejszner, L., 1856. Über eine Längenmoräne im Thale des Biały Dunajec bei dem Hochofen von Zakopane in der Tatra. Sitz. Kais. Akad. Wiss. Wien Math.-Naturwiss 1 (21), 259–262.
Zreda, M., Phillips, F.M., 1995. Insights into alpine moraine development from cosmogenic ^{36}Cl build up dating. Geomorphology 14 (2), 149–156.
Zreda, M.G., Phillips, F.M., Elmore, D., 1994. Cosmogenic ^{36}Cl accumulation in unstable landforms 2. Simulations and measurements on eroding moraines. Water Resour. Res. 30 (11), 3127–3136.
Zumbühl, H.J., Steiner, D., Nussbaumer, S.V., 2008. 19th century glacier representations and fluctuations in the central and western European Alps: an interdisciplinary approach. Glob. Planet. Change 60 (1–2), 42–57.